JOC The Journal of Organic Chemistry

pubs.acs.org/joc Article

Unusual Oxidative Dealkylation Strategy toward Functionalized Phenalenones as Singlet Oxygen Photosensitizers and Photophysical Studies

Paul De Bonfils, Elise Verron, Catalina Sandoval-Altamirano, Pablo Jaque, Xavier Moreau, German Gunther, Pierrick Nun, and Vincent Coeffard*

Cite This: J. Org. Chem. 2020, 85, 10603−10616 Read Online

ACCESS | Metrics & More | Article Recommendations | Supporting Information

ABSTRACT: A series of functionalized 6-alkoxy phenalenones was prepared through an unprecedented oxidative dealkylation of readily available phenalene precursors. The starting phenalenes were efficiently synthesized *via* an aminocatalyzed annulation/*O*-alkylation strategy starting from simple substrates. The spectroscopic properties of some phenalenones were investigated in different solvents. Introducing an alkoxy substituent at the 6-position onto the phenalenone framework results in a red shift of the absorption. The synthesized phenalenones exhibit low fluorescence quantum yields, and the fluorescence decay was studied in different solvents, highlighting the presence of several lifetimes. The singlet oxygen ($^1O_2$) photosensitizing propensity of some phenalenones was investigated, and the results showed the striking importance of the phenalenone molecular structure in generating singlet oxygen with high yields. The ability of phenalenones to generate singlet oxygen was then harnessed in three photooxygenation reactions: anthracene oxidation, oxy-functionalization of citronellol through the Schenck-ene reaction, and photooxidation of a diene.

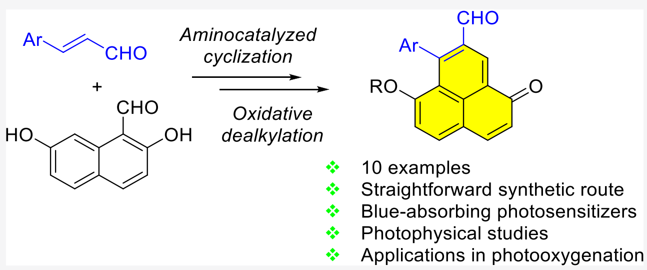

■ INTRODUCTION

The light-induced production of reactive oxygen species lies at the heart of photodynamic therapy (PDT). Over the past decades, this research field has been thriving with applications ranging from the treatment of superficial cancers[1] to the destruction of bacteria,[2] fungi,[3] or viruses.[4] The concept of PDT is based on the combination of oxygen, light, and a photosensitizer (PS). The classical mechanism starts with the activation of PS through light absorption to initially generate its excited singlet state, which would then evolve to the excited triplet state by intersystem crossing.[5] The photosensitizer in its triplet state can subsequently react with molecular entities to form radical or radical ions, leading to the oxidized and/or oxygenated products (type-I photooxygenation) or can generate singlet oxygen by triplet−triplet energy transfer (type-II photooxygenation).[6] One convenient strategy to enhance intersystem crossing lies in the incorporation of heavy atoms (i.e., Ir, Ru, Pd, I, Br) into the PS.[7] Nevertheless, the dark toxicity and cost of heavy-atom-containing PSs are drawbacks to fully exploit the potential of PDT in clinical applications. Within this context, the cost-effective development of organic PSs deprived of heavy atoms is of utmost importance to tackle the challenge of efficient production of singlet oxygen by sensitization of ground-state oxygen.[8] One approach in which these demands can be achieved is through the use of phenalenone derivatives. Phenalenone is a type-II PS, which is considered as a universal reference molecule for the determination of quantum yields of singlet oxygen sensitization.[9] Phenalenone possesses attractive features for singlet oxygen production such as its photostability in various solvents, an efficient intersystem crossing, and a high quantum yield of singlet oxygen.[10] These interesting features have spurred interest in investigating phenalenone compounds as prospective PDT agents.[11] In addition, the phenalenone framework is also found in biologically relevant products exhibiting antileishmanial,[12] antifungal,[13] and antimalarial activities.[14] However, the drawbacks of phenalenones such as their tendency to aggregate,[11f,15] absorption in UVA regions, and limited synthetic strategies to obtain functionalized structures still constitute important barriers to their widespread adoption. An approach to circumventing these issues lies in the molecular design of new visible-light-absorbing phenalenone architectures thoroughly decorated with functional groups. From a synthetic standpoint, a convenient route toward

Received: May 14, 2020
Published: July 3, 2020

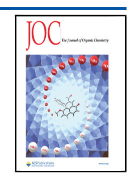

Downloaded via UNIV DE CHILE on November 6, 2020 at 00:58:23 (UTC).
See https://pubs.acs.org/sharingguidelines for options on how to legitimately share published articles.

ACS Publications © 2020 American Chemical Society

phenalenones involves the reaction of naphthalene compounds with acrylic acid or derivatives followed by an oxidative protocol (Scheme 1).[16] The Lewis-acid-promoted reaction of naphthalic anhydride and diethyl malonate compounds has also been reported as an efficient procedure to give access to phenalenones, but this strategy remains limited in terms of substrate scope.[17]

Scheme 1. Designed Phenalenone Photosensitizers PSs and Synthetic Strategies

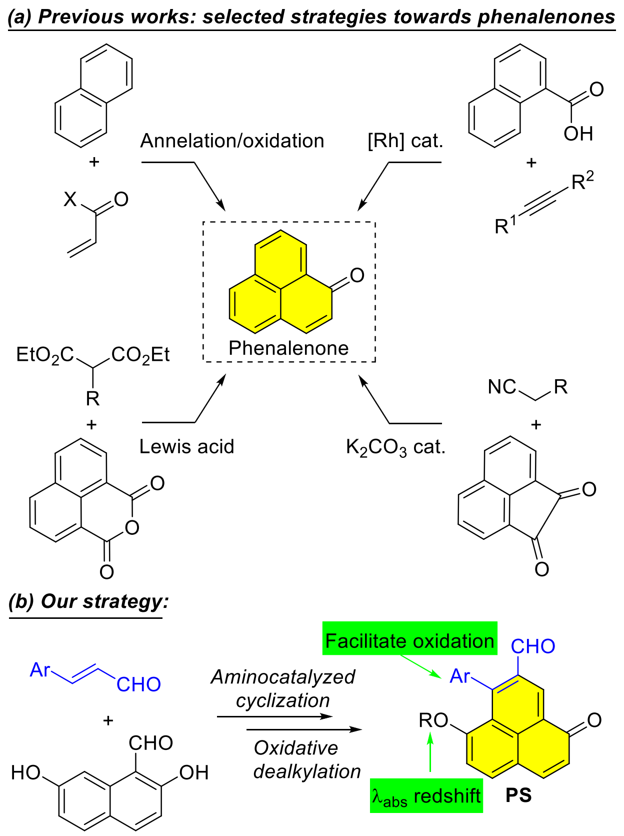

More recently, the group of Fukuyama described the preparation of phenalenones through a rhodium-catalyzed dehydrative annulation of 1-naphthoic acids with alkynes.[18] Methylene active compounds bearing a cyano group have also been used by Lebreton and co-workers for the preparation of phenalenones from acenaphthylene-1,2-dione.[19] Nevertheless, this attractive synthetic route was limited to unsubstituted naphthalene ring-containing substrates. In spite of substantial efforts toward the preparation of phenalenone architectures, the current strategies have several drawbacks such as lengthy multistep routes or limited ability to introduce functional groups onto the phenalenone frameworks.[20] We described herein a synthetic strategy toward highly promising phenalenone PSs with high singlet oxygen quantum yields *via* an oxidative dealkylation tactic.

■ RESULTS AND DISCUSSION

Synthesis. We began our study by preparing a series of phenalene derivatives **4** following the synthetic route depicted in Scheme 2. The reaction sequence started with the condensation of naphthol **1**[21] with a series of *α*,*β*-unsaturated aldehydes **2** in the presence of a catalytic amount of triethylamine (5 mol %) and a racemic mixture of diphenylprolinol silyl ether catalyst (20 mol %). This procedure is based on a slightly modified experimental protocol previously reported by our group.[22] The yields were improved by simply switching the solvent from toluene to ethyl acetate. Under these conditions, the products **3** were obtained in good to high yields regardless of the substituents. Nevertheless, the introduction of a dimethylamino group on the aryl ring of the *α*,*β*-unsaturated aldehyde **2j** had a dramatic impact on the reaction outcome and only a small amount of **3j** was detected in the crude product. It is worthwhile noting that

Scheme 2. Synthetic Route toward Phenalene Derivatives[a]

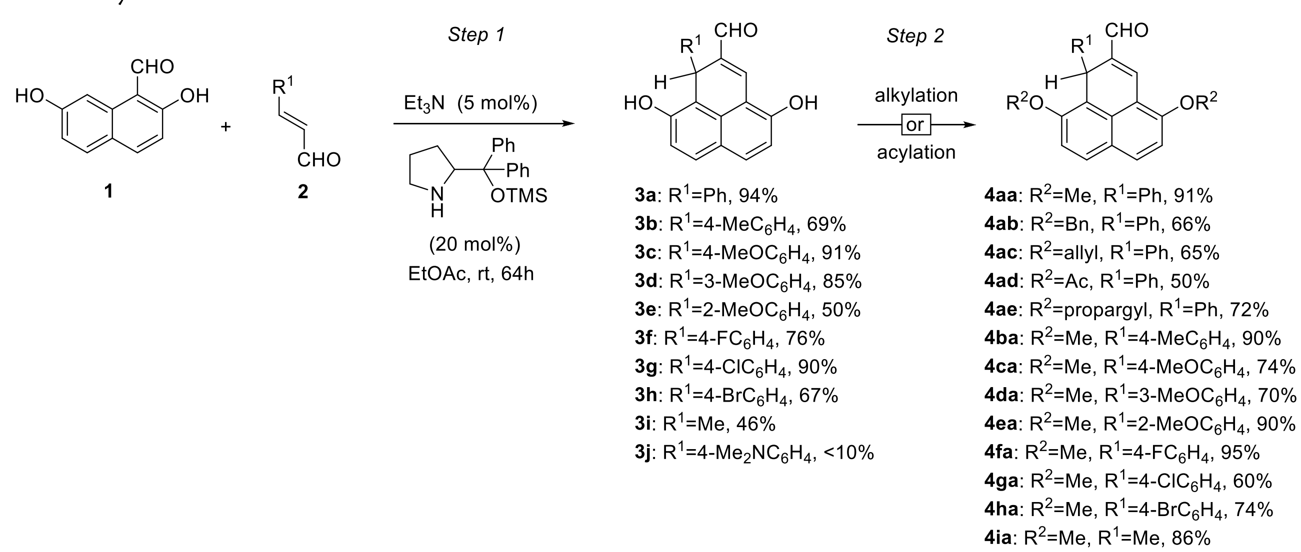

[a]Reaction conditions. Step 1, reactions were performed in ethyl acetate (5 mL, 0.20 mol L^{-1}) at room temperature for 64 h using 2 equiv of **2**, 5 mol % Et_3N, and 20 mol % diphenylprolinol silyl ether catalyst. Step 2, methylation: MeI (2.2 equiv), K_2CO_3, dimethylformamide (DMF), rt, 5 h. Benzylation: BnBr (2.5 equiv), K_2CO_3, acetone, reflux, 5 h. Allylation: allyl bromide (4 equiv), K_2CO_3, acetone, reflux, 5 h. Acylation: acetic anhydride (4 equiv), pyridine, rt, 5 h. Propargylation: propargyl bromide (5 equiv), K_2CO_3, acetone, reflux, 16 h.

https://dx.doi.org/10.1021/acs.joc.0c01140
J. Org. Chem. 2020, 85, 10603−10616

aminocatalyzed transformation between **1** and *trans*-cinnamaldehyde **2a** (R^1 = Ph) was scaled up to 10 mmol and proceeded with excellent yield (90%). With the compounds **3** in hand, the *O*-alkylation and *O*-acylation were investigated. Methylation, benzylation, and allylation reactions gave rise to the *O*-protected phenalenes in good to excellent yields, while **3a** was acylated in the presence of acetic anhydride in pyridine to give **4ad** in 50% yield.

To identify suitable conditions for the oxidative dealkylation,[23] the transformation of **4aa** into the corresponding phenalenones **5** and **5′** was investigated (Table 1).

Table 1. Oxidant Screening

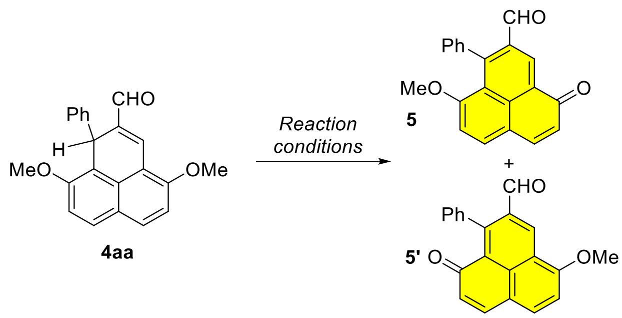

entry	reaction conditions	yield 5/5′[a]
1	DDQ (2 equiv), CH_2Cl_2, 1 h, rt	47%/49%
2	$NOBF_4$ (2 equiv), MeCN, 1 h, rt	32%/66%
3	MnO_2 (20 equiv), CH_2Cl_2, 60 h, rt	31%/8%
4	MnO_2 (20 equiv), CH_2Cl_2, 96 h, rt	50%/20%
5	MnO_2 (20 equiv), CH_2Cl_2, 48 h, reflux	27%/5%

[a]Isolated yield.

The oxidant 2,3-dichloro-5,6-dicyano-1,4-benzoquinone (DDQ) has been successfully used in oxidative dealkylation and therefore we first explored this oxidant (entry 1).[23a] Oxidation of **4aa** in dichloromethane with 2 equiv of DDQ led to the formation of two phenalenone compounds **5** and **5′** in 47 and 49% isolated yields, respectively. It is important to note that full NMR analyses were carried out to unambiguously confirm the structures of **5** and **5′**, which were easily separated by column chromatography. The promising results prompted us to explore some oxidants to improve the reaction selectivity. The use of nitrosyl tetrafluoroborate ($NOBF_4$) at room temperature provided **5′** as the major compound in 66% yield, while **5** was isolated in 32% yield (entry 2). Nevertheless, recent studies have shown that 9-phenylsubstituted phenalenones such as **5′** were inefficient photocatalysts for oxygen sensitization due to a competitive reaction pathway.[24] Changing the oxidant to MnO_2 enhanced the selectivity toward the major formation of **5** (entries 3−5). The use of MnO_2 in dichloromethane at room temperature provided an effective balance between yield in **5** and selectivity (entry 4). Having identified suitable conditions for the phenalenone formation, we investigated the scope and limitations of the transformation (Scheme 3).

Phenalene compounds **4** (R^1 = Ph) bearing *O*-alkylated groups on the naphthalene ring were well tolerated, and the desired phenalenones **5**−**8** were obtained in 50−55% isolated yields with good selectivities. In contrast, the oxidation of **4ad** (R^1 = Ph, R^2 = Ac) led to the formation of the corresponding phenalenone, which was unstable upon purification by column chromatography on silica gel. A similar reaction outcome was

Scheme 3. Substrate Scope

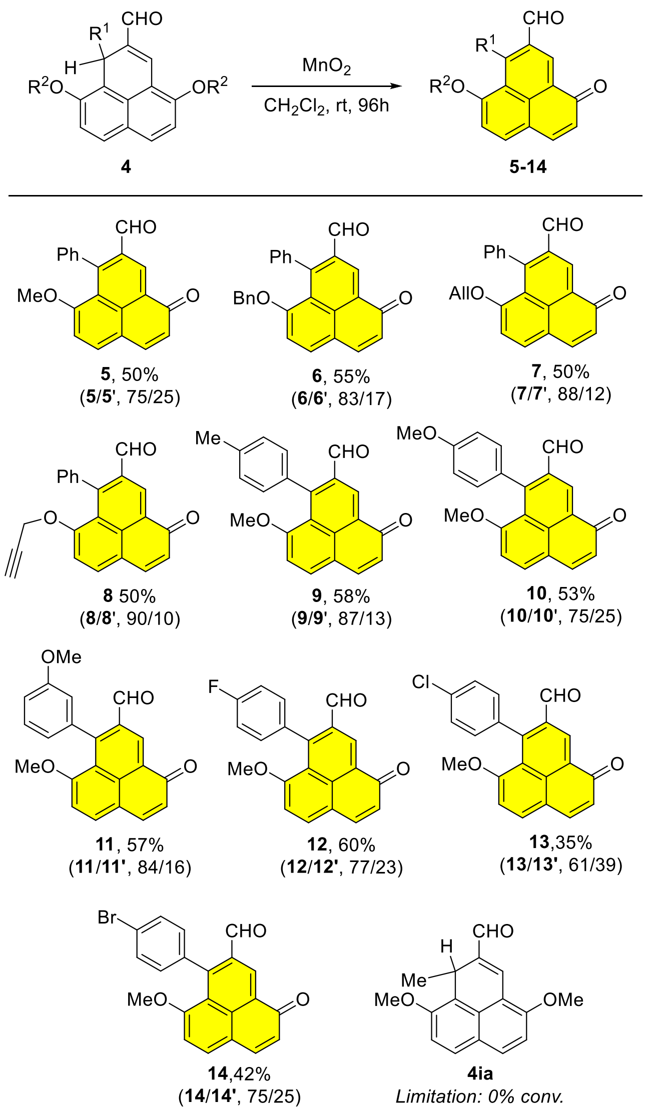

observed by performing the oxidation of phenalene **4ea** (R^1 = 2-$MeOC_6H_4$, R^2 = Me). The use of *O*-alkylated phenalene derivatives as substrates is crucial for the success of the reaction because running the reaction with **3a** led to a complete degradation of the starting material. The phenalene substrates incorporating different substituents on the phenyl ring were prone to oxidation. The compounds **9**−**12** were isolated in 53−60% yields, while products **13** and **14** were formed with moderate levels of yields. The methyl-derived phenalene **4ia** was subjected to the standard reaction conditions, and no oxidation was observed. This result underscores the importance of the aromatic substituent R^1 to trigger the oxidative dealkylation. Although a comprehensive understanding of the mechanism should await further investigations, cyclic voltammetry of phenalene **4aa** was performed (Figure 1).

The cyclic voltammogram of **4aa** showed an irreversible electron oxidation process with a peak potential at $E_{p,a}$ = 1.27 V (vs SCE), which correlates with the oxidation ability of MnO_2.[25] A set of control experiments was performed to get a better understanding of the formation of phenalenones from phenalenes **4** (Scheme 4).

https://dx.doi.org/10.1021/acs.joc.0c01140
J. Org. Chem. 2020, 85, 10603−10616

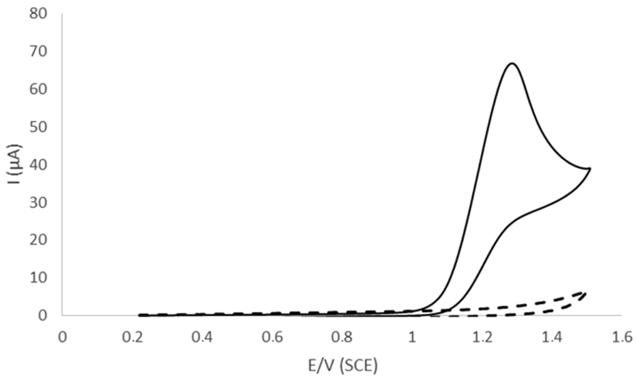

Figure 1. Cyclic voltammogram at a glassy carbon electrode in dichloromethane and Bu_4NPF_6, c = 0.1 mol L^{-1} referenced to saturated calomel electrode (SCE) *via* internal ferrocene (not shown) (---) and in the presence of **4aa** (—), $c = 5 \times 10^{-3}$ mol L^{-1}, 100 mV s^{-1}.

Scheme 4. Control Experiments[a]

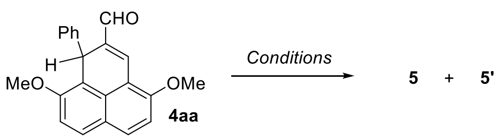

[a]*t*BuLi or NaH (1.2 equiv), THF, 0 °C to room temperature (RT): no reaction. Ph_3CBF_4 (1.2 equiv), MeCN, RT to reflux: no reaction. *N*-Bromosuccinimide (NBS; 2 equiv), azobisisobutyronitrile (AIBN; 0.1 equiv), 1,2-DCE, reflux: **5** (2%), **5′** (2%).

First, phenalene **4aa** was treated with strong bases under an inert atmosphere to assess whether a phenalenyl anion could be an intermediate of the reaction.[26] No reaction occurred under these conditions, and the starting material **4aa** was recovered. With the aim of preparing the phenalenyl cation, **4aa** was allowed to react with tritylium tetrafluoroborate according to a known procedure.[27] Even under reflux conditions, no traces of the desired phenalenones **5** and **5′** were detected. Gratifyingly, the expected phenalenones **5** and **5′** were detected by treating the phenalene **4aa** under radical conditions using *N*-bromosuccinimide (NBS) and azobisisobutyronitrile (AIBN). Therefore, the formation of phenalenones from phenalene **4** could proceed through a radical intermediate.

Spectroscopic properties of phenalenones **5** and **5′** were investigated to study the influence of the substitution pattern.

Spectroscopic Characterization. *Steady-State Absorption and Emission Spectra.* The absorption spectra in MeOH of phenalenone (**PN**), **5**, and **5′** as representative derivatives are presented in Figure 2. The absorption spectra of **5**/**5′** and **PN** show noticeable differences. The group of absorption

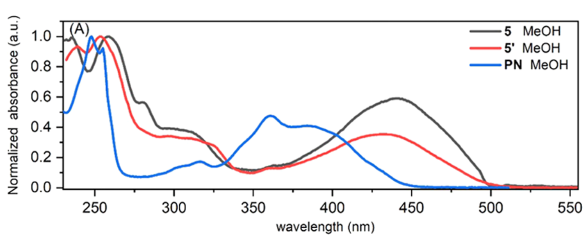

Figure 2. Absorption spectra of phenalenone (**PN**), **5**, and **5′** in methanol.

bands located between 330 and 360 nm, ascribed for phenalenone to a $\pi\pi^*$ transition, are weak in derivatives **5**/**5′**. The band related to $n\pi^*$ transition was displaced to a longer wavelength (430–450 nm), and these results are in agreement with previous studies dealing with photophysical analyses of 6-ethoxy and 6-hydroxy phenalenones.[28]

The molar extinction coefficients (ε) determined for **5** and **5′** in several solvents are shown in Table 2. A longer wavelength absorption and higher ε values were determined for **5**. Additionally, a bathochromic shift is observed in the absorption wavelength with the increase of solvent polarity for this compound.

Table 2. Molar Extinction Coefficients Determined in Selected Solvents (ε, 10^3 M^{-1} cm^{-1})

	5	5′
solvent	$\varepsilon/10^3$ M^{-1} cm^{-1} (λ_{max}/nm)	$\varepsilon/10^3$ M^{-1} cm^{-1} (λ_{max}/nm)
cyclohexane	12.23 (419)	8.29 (412)
toluene	10.49 (425)	8.06 (426)
chloroform	11.86 (436)	8.19 (431)
acetonitrile	10.11 (435)	8.74 (426)
methanol	11.31 (442)	8.31 (431)

Normalized emission spectra of **5** and **5′** in several solvents are shown in Figure 3. The maximum emission wavelength is dependent on the solvent polarity in both derivatives, and the higher shift is observed in protic polar media. The emission intensity of compound **5′** was lower than that observed for **5** in all solvents. Investigations of excited singlet-state properties in apolar solvents were not carried out because emission was very low.

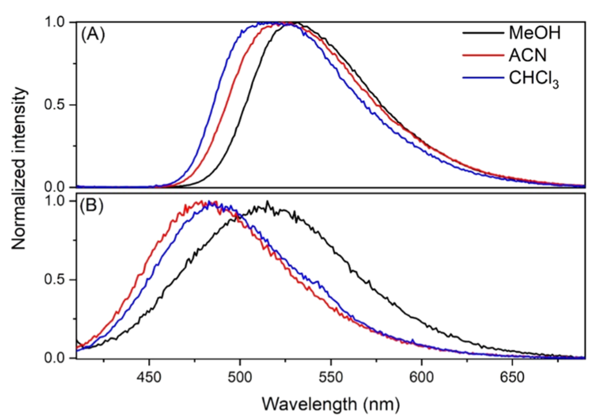

Figure 3. Normalized emission spectra in several solvents for **5** (A) and **5′** (B). λ_{exc} = 360 nm.

Fluorescence quantum yields measured under air ($\Phi_{F,air}$) and under argon ($\Phi_{F,Ar}$) for **5** and **5′** are shown in Table 3. Besides being low, the similarity between values indicates that oxygen is not able to quench appreciably the singlet states of these derivatives. Both the emission quantum yields and emission maximum wavelengths are sensitive to the polarity solvent, and the bathochromic effect observed indicates $n\pi^*$ character for the transition involved.

Time Resolved Measurements. Fluorescence lifetime data were analyzed by global fitting of a set of decays acquired at different emission wavelengths. A representative data analysis showing a biexponential fit for phenalenone **5** in methanol is

https://dx.doi.org/10.1021/acs.joc.0c01140
J. Org. Chem. 2020, 85, 10603−10616

Table 3. Quantum Yields of Fluorescence in Selected Solvents

	5		5′	
solvent	$\Phi_{F,air}$	$\Phi_{F,Ar}$	$\Phi_{F,air}$	$\Phi_{F,Ar}$
chloroform	0.034 ± 0.003	0.030 ± 0.001	0.003 ± 0.0005	0.004 ± 0.001
acetonitrile	0.031 ± 0.006	0.042 ± 0.003	0.004 ± 0.001	0.004 ± 0.0007
methanol	0.225 ± 0.010	0.280 ± 0.007	0.007 ± 0.002	0.009 ± 0.001

shown in Figure 4, and the inset of the figure shows time-resolved emission spectra (TRES) with two bands centered at around 540 nm. Three bands (two centered at around 530 nm and one centered at 490 nm) were observed in the TRES for **5′** in methanol (see Figure S3 in the Supporting Information).

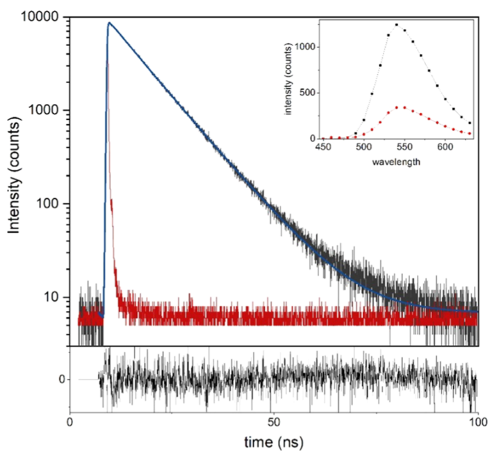

Figure 4. Emission decay of **5** in methanol at 520 nm (λ_{exc} = 375 nm) under air. The inset corresponds to time-resolved fluorescence spectra (pre-exponential factors obtained from a global fit of fluorescence intensity time traces).

Regardless of the solvent, phenalenone **5** shows two fluorescent lifetimes (Table 4), while **5′** has three lifetimes (see Table S2 in the Supporting Information). In all cases, the saturation of a solution with argon did not influence the lifetime values even if a small change in lifetimes was observed in some cases.

Table 4. Fluorescence Lifetime of 5 in Selected Solvents[a]

	5			
solvent	$\tau_{1,air}$/ns	$\tau_{2,air}$/ns	$\tau_{1,Ar}$/ns	$\tau_{2,Ar}$/ns
chloroform	5.88 (1.2)	0.85 (98.8)	8.35 (7.4)	0.77 (92.3)
acetonitrile	7.71 (5.7)	1.07 (94.3)	8.46 (6.8)	1.06 (93.2)
methanol	8.80 (76.1)	6.12 (23.9)	8.56	

[a]The values in parenthesis correspond to fractional intensities of lifetimes.

The presence of multiexponential decays observed for the emission of both compounds **5** and **5′** can be explained through the participation of rotamers involving both the aldehyde moiety and the phenyl ring (Figure 5). Density functional theory (DFT) and time-dependent DFT (TD-DFT) calculations were performed on phenalenones **5** and **5′** at the B3LYP and CAM-B3LYP levels, respectively.

The interconversion between the stable conformers is kinetically and thermodynamically feasible in both cases accordingly with the activation free energy and the thermodynamic driving force values at the ground and excited

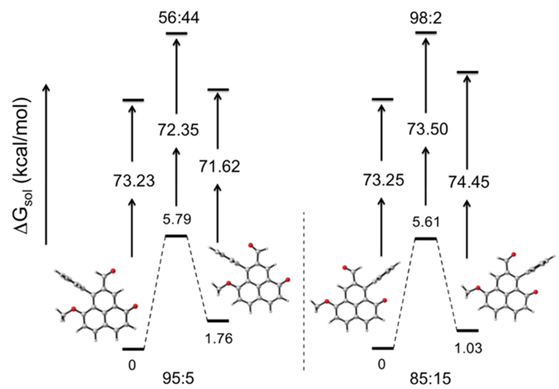

Figure 5. DFT (TD-DFT)-computed energy surfaces for the conformational change of **5** (left) and **5′** (right) in their ground (excited) states. Vertical excitation energies provided by TD-DFT calculations are also depicted in the figure.

states. By taking into account the thermodynamic driving force data, the following ratios between the stable conformers of 95:5 (56:44) and 85:15 (98:2) are computed for **5** and **5′** derivatives in their ground (excited) states. These data suggest that both isomers would be present in solution under the experimental conditions and both of them could be prone to be excited. This result could explain the different lifetimes measured in methanol for both phenalenone derivatives.[29]

Singlet Oxygen Generation. Singlet oxygen quantum yields (Φ_Δ) were determined by observing the 1270 nm emission of $^1O_2$ of air-saturated samples excited at 355 nm. The results indicate that the solvent highly modulates the capacity of the studied compounds **5** and **5′** to generate $O_2(^1\Delta_g)$ (Table 5).

Table 5. Singlet Oxygen Quantum Yields of Compounds 5 and 5′[a]

	5	5′
solvent	$\Phi_{\Delta,air}$	$\Phi_{\Delta,air}$
cyclohexane	1.09	0.52
toluene	1.17	0.21
chloroform	0.53	0.13
acetonitrile	0.72	0.22
methanol	0.38	0.22

[a]The values were determined using phenalenone as an actinometer. λ_{exc} = 355 nm.

For phenalenone **5**, the lowest singlet oxygen quantum yield values were obtained in methanol and chloroform. Particularly, in methanol, hydrogen-bonding interactions could promote a lowered ISC, as reported by Martínez et al. for 9*H*-fluoren-9-one.[30] This result is fully consistent with the higher fluorescence quantum yield and singlet excited-state lifetime determined in this solvent. On the other hand, the compound **5′** presents lower singlet oxygen quantum yields and with the exception of cyclohexane almost independent of the solvent. In

https://dx.doi.org/10.1021/acs.joc.0c01140
J. Org. Chem. 2020, 85, 10603−10616

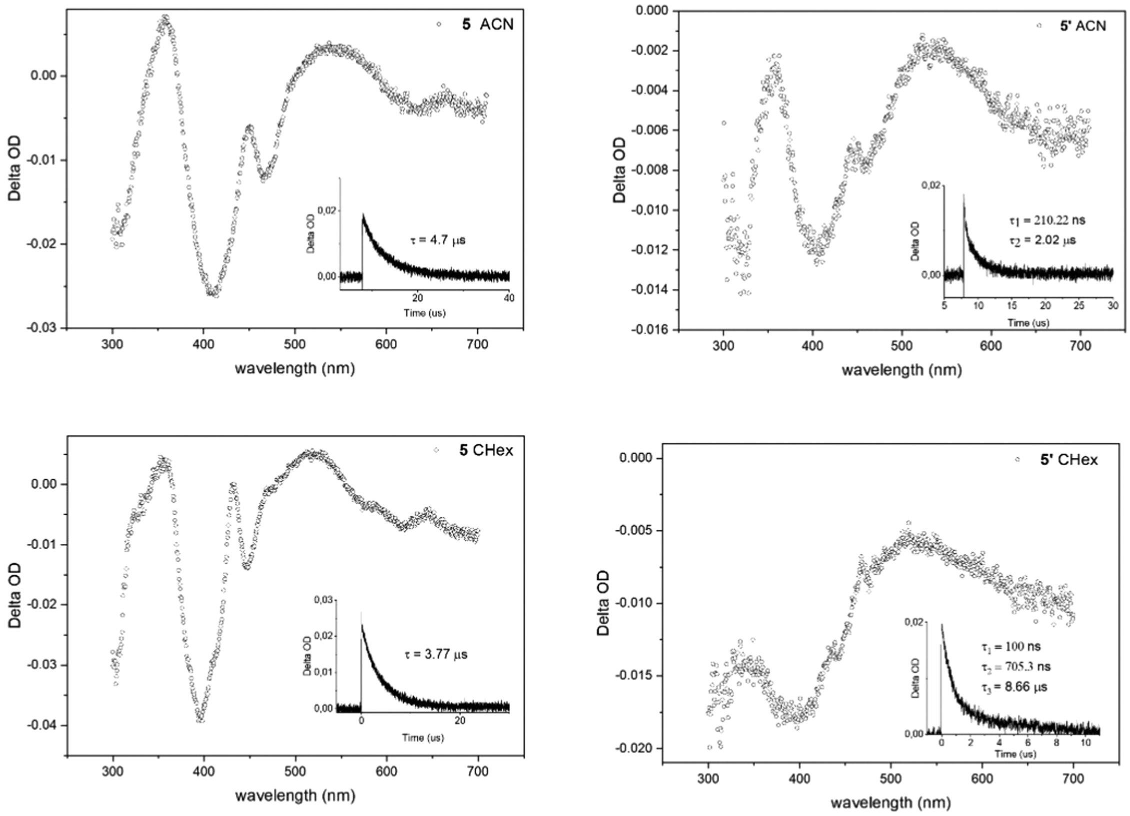

Figure 6. Triplet−triplet absorption spectra of **5** and **5′** in acetonitrile and cyclohexane acquired after a 100 ns pulse. The insets show the kinetic traces at around 530 nm.

light of the very low singlet oxygen quantum yield for this compound the main deactivation path would correspond to internal conversion.

Laser Flash Photolysis Absorption Experiments. Triplet−triplet absorption experiments in argon-saturated acetonitrile and cyclohexane solutions were performed for both derivatives. The transient decays for **5** were monoexponential in both solvents studied (decays followed at 550 nm in acetonitrile and 530 nm in cyclohexane). This result is consistent with the absorption of only one species, which additionally is strongly quenched by oxygen, and almost disappeared when oxygen was admitted to the samples. Therefore, the observed transient absorptions should be attributed to the excited triplet state of **5**. For both derivatives, the transient spectra are similar, showing four absorption bands and a ground depletion (Figure 6). For phenalenone **5**, three absorption maxima appear at 350, 540, and 650 nm with a lifetime of 4.7 ± 0.06 μs in acetonitrile and 3.8 ± 0.07 μs in cyclohexane. Additionally, ground depletion and emission are observed at 410 and 469 nm. The estimation of ε cannot be done for the absorption bands below 500 nm due to the ground-state absorption. For compound **5′**, similar absorption peaks and ground depletion/emission were observed in acetonitrile. Nevertheless, the signals are clearly of a lower magnitude, indicating (if extinction coefficients of transients are similar) a lower production of transient states, compatible with the behavior described previously for singlet oxygen quantum yields. The decay at 540 nm in acetonitrile fits to a biexponential, where probably the longer component (2.0 μs corresponds to the triplet state), while in cyclohexane there are three components, and the triplet state could have a lifetime of 0.7 or 8.7 μs. All components disappear in the presence of oxygen regardless of the solvents.

Photooxygenation. Phenalenones have been scarcely investigated as photosensitizers in synthetic transformations in spite of their ability to generate singlet oxygen in high yields. In light of the photophysical studies, the phenalenone compound **5** has been tested as a photosensitizer (Scheme 5). The photooxygenation reactions have been performed under oxygen bubbling or under atmospheric pressure of oxygen by utilizing blue light (light-emitting device (LED), λ = 470 nm).

Photooxygenation of anthracene **15**, which is a singlet oxygen trap, was first investigated.[31] Irradiation of **15** in the presence of 2 mol % **5** led to the quantitative production of anthracene-9,10-endoperoxide **16** and **5**, which turned out to be stable under the reaction conditions. Other photosensitizers such as **10** or **12** (2 mol %) were tested in the photooxygenation of **15**, and full conversions into **16** were also observed after 1 h. Photooxidation of citronellol **17**, which is a key step in the industrial production of the fragrance rose oxide, was then explored. The singlet oxygen Schenck-ene reaction of **17** was performed in chloroform under blue light using 2 mol % phenalenone **5**. Subsequent reductive work led to an equimolar mixture of allylic alcohols **18a** and **18b** in 70% overall yield. The photosensitizer **5** was also effective for the formation of endoperoxides through [4 + 2] cycloaddition. Photooxygenation of cyclohexa-1,3-diene **19** in the presence of a catalytic amount of **5** followed by reduction with thiourea led to the formation of the diol **20** in 90% yield.

■ CONCLUSIONS

In summary, functionalized phenalenone derivatives were prepared based on an unusual oxidative dealkylation as a key

Scheme 5. Application of PS 5 in Singlet-Oxygen-Mediated Transformations

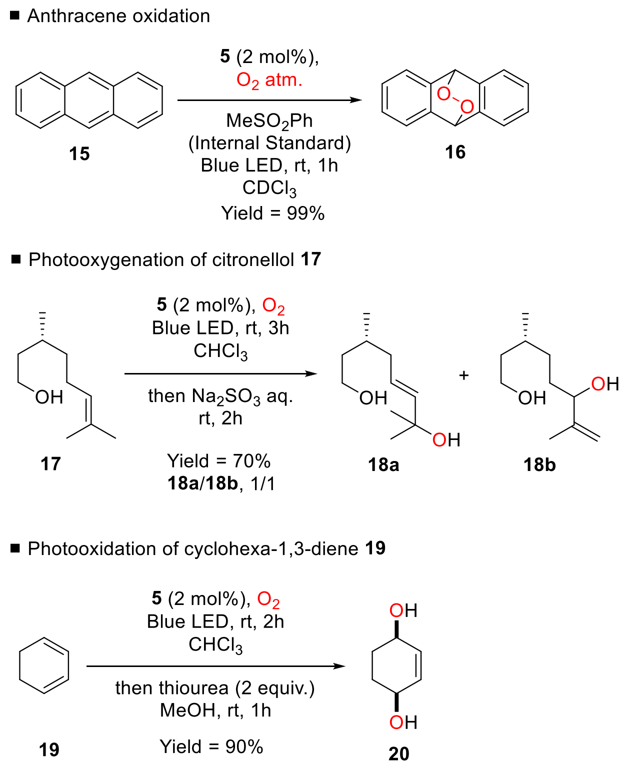

step. A protocol has been implemented to synthesize functionalized phenalenones from readily available phenalenes with a simple oxidant and practically straightforward reaction conditions. A red shift absorption was observed, owing to the insertion of an alkoxy group at the 6-position on the phenalenone ring. Singlet excited-state deactivation of these derivatives is mainly controlled by nonradiative processes: intersystem crossing to the triplet excited state or internal conversion to a ground-state singlet. Transients with a triplet character were observed by flash photolysis for all compounds studied determining their lifetimes. The phenalenone derivatives studied show deactivation pathways dependent on the substituent position, keeping in one case a high capacity of singlet oxygen generation, which is the most remarkable property of phenalenone. A computational study predicts a feasible rotameric equilibrium in both derivatives in methanol. The propensity of phenalenone motifs to generate singlet oxygen under light irradiation prompted us to investigate their use as photosensitizers in photooxygenation reactions. Under a blue light LED, phenalenone photosensitizers were successfully applied to endoperoxide formation and Schenck-ene reactions. Investigations are ongoing to further harness the biological and synthetic potential of these phenalenones as photosensitizers.

■ EXPERIMENTAL SECTION

Materials and Methods. ^{1}H NMR and ^{13}C spectra were recorded at room temperature on samples dissolved in $CDCl_3$. Chemical shifts (δ) are given in parts per million, and coupling constants are given as absolute values expressed in hertz. Structural assignments were made with additional information from gCOSY, gHSQC, and gHMBC experiments. High-resolution mass spectrometry (HRMS) analyses were performed using electrospray ionization (ES) and ASAP. FTIR spectra were recorded from neat samples using the attenuated total reflection (ATR) technique. Thin-layer chromatography (TLC) was carried out on aluminum sheets precoated with silica gel. Column chromatography separations were performed using silica gel. All reagents were used without purification. All solvents were of HPLC grade or were distilled using standard drying agents prior to use. Starting chemical substrates and reagents were used as commercially provided unless otherwise indicated.

Synthetic Procedures. *Synthesis of Phenalene Derivatives (3a–i).* The naphthalene substrate (1 equiv) was introduced into a capped flask. Ethyl acetate (0.2 mol L^{-1}), a racemic mixture of diphenylprolinol silyl ether catalyst (20 mol %), and the α,β-unsaturated aldehyde (2 equiv) were successively added into the flask. Et_3N (5 mol %) was then added, and the resulting mixture was stirred at room temperature for 64 h at which point the solvent was removed under reduced pressure. The crude compound was purified by column chromatography on silica gel to afford the corresponding product.

*4,9-Dihydroxy-1-phenyl-1H-phenalene-2-carbaldehyde (**3a**).* According to the described general procedure, 1.51 g (94%) of **3a** (orange solid) was obtained from 2,7-dihydroxy-1-naphthtaldehyde (5.32 mmol, 1 g), catalyst (1.06 mmol, 345 mg), cinnamaldehyde (10.62 mmol, 1.34 mL), and Et_3N (0.27 mmol, 37 μL). The compound was purified by column chromatography on silica gel (6/4 PE/EtOAc). All of the physical and spectroscopic data were in complete agreement with the reported ones.[22]

*4,9-Dihydroxy-1-(p-tolyl)-1H-phenalene-2-carbaldehyde (**3b**).* According to the described general procedure, 350 mg (69%) of **3b** (orange solid) was obtained from 2,7-dihydroxy-1-naphthtaldehyde (1.59 mmol, 300 mg), catalyst (0.32 mmol, 104 mg), (*E*)-3-(*p*-tolyl)acrylaldehyde (3.18 mmol, 465 mg), and Et_3N (79.5 μmol, 11 μL). The compound was purified by column chromatography on silica gel (8/2 PE/EtOAc). R_f = 0.31 (PE/EtOAc 8/2). Mp 210–212 °C. ^{1}H NMR (300 MHz, acetone-d_6) δ 2.16 (s, 3H), 5.65 (s, 1H), 6.91–6.88 (m, 2H), 6.97 (d, J = 8.7 Hz, 1H), 7.05 (d, J = 8.9 Hz, 1H), 7.13–7.10 (m, 2H), 7.55 (d, J = 8.7 Hz, 1H), 7.55 (d, J = 8.9 Hz, 1H), 8.00 (s, 1H), 9.60 (s, 1H). ^{13}C{^{1}H} NMR (75 MHz, acetone-d_6) δ 20.9, 38.8, 113.2, 115.9, 116.8, 119.3, 123.8, 128.5, 129.0, 129.1 (2C), 132.0 (2C), 133.9, 135.9, 139.0, 139.2, 143.1, 154.9, 155.2, 192.1. IR (ATR, cm^{-1}) 3498, 3187, 2917, 1735, 1277, 1157. HRMS (ES+) m/z: [M + Na]$^+$ calcd for $C_{21}H_{16}NaO_3$ 339.0997; found 339.1001.

*4,9-Dihydroxy-1-(4-methoxyphenyl)-1H-phenalene-2-carbaldehyde (**3c**).* According to the described general procedure, 800 mg (91%) of **3c** (red solid) was obtained from 2,7-dihydroxy-1-naphthtaldehyde (2.65 mmol, 500 mg), catalyst (0.53 mmol, 173 mg), (*E*)-3-(4-methoxyphenyl)acrylaldehyde (5.31 mmol, 860 mg), and Et_3N (0.13 mmol, 18 μL). The compound was purified by column chromatography on silica gel (6/4 PE/EtOAc). All of the physical and spectroscopic data were in complete agreement with the reported ones.[22]

*4,9-Dihydroxy-1-(3-methoxyphenyl)-1H-phenalene-2-carbaldehyde (**3d**).* According to the described general procedure, 810 mg (85%) of **3d** (red solid) was obtained from 2,7-dihydroxy-1-naphthtaldehyde (2.65 mmol, 500 mg), catalyst (0.53 mmol, 173 mg), (*E*)-3-(3-methoxyphenyl)acrylaldehyde (5.3 mmol, 860 mg), and Et_3N (0.13 mmol, 18 μL). The compound was purified by column chromatography on silica gel (6/4 PE/EtOAc). All of the physical and spectroscopic data were in complete agreement with the reported ones.[22]

*4,9-Dihydroxy-1-(2-methoxyphenyl)-1H-phenalene-2-carbaldehyde (**3e**).* According to the described general procedure, 132 mg (50%) of **3e** (red solid) was obtained from 2,7-dihydroxy-1-naphthtaldehyde (0.78 mmol, 147 mg), catalyst (0.16 mmol, 52 mg), (*E*)-3-(2-methoxyphenyl)acrylaldehyde (1.56 mmol, 253 mg), and Et_3N (39 μmol, 5 μL). The compound was purified by column chromatography on silica gel (6/4 PE/EtOAc). All of the physical and spectroscopic data were in complete agreement with the reported ones.[22]

*1-(4-Fluorophenyl)-4,9-dihydroxy-1H-phenalene-2-carbaldehyde (**3f**).* According to the described general procedure, 389 mg (76%) of **3f** (orange solid) was obtained from 2,7-dihydroxy-1-naphthtaldehyde (1.59 mmol, 300 mg), catalyst (0.32 mmol, 104

https://dx.doi.org/10.1021/acs.joc.0c01140
J. Org. Chem. 2020, 85, 10603–10616

mg), (*E*)-3-(4-fluorophenyl)acrylaldehyde (3.18 mmol, 0.42 mL), and Et_3N (79.5 μmol, 11 μL). The compound was purified by column chromatography on silica gel (7/3 PE/EtOAc). All of the physical and spectroscopic data were in complete agreement with the reported ones.[22]

*1-(4-Chlorophenyl)-4,9-dihydroxy-1H-phenalene-2-carbaldehyde (**3g**).* According to the described general procedure, 482 mg (90%) of **3g** (orange solid) was obtained from 2,7-dihydroxy-1-naphthtaldehyde (1.59 mmol, 300 mg), catalyst (0.32 mmol, 104 mg), (*E*)-3-(4-chlorophenyl)acrylaldehyde (3.18 mmol, 530 mg), and Et_3N (79.5 μmol, 11 μL). The compound was purified by column chromatography on silica gel (7/3 PE/EtOAc). All of the physical and spectroscopic data were in complete agreement with the reported ones.[22]

*1-(4-Bromophenyl)-4,9-dihydroxy-1H-phenalene-2-carbaldehyde (**3h**).* According to the described general procedure, 294 mg (67%) of **3h** (orange solid) was obtained from 2,7-dihydroxy-1-naphthtaldehyde (1.16 mmol, 218 mg), catalyst (0.23 mmol, 75 mg), (*E*)-3-(4-bromophenyl)acrylaldehyde (2.32 mmol, 490 mg), and Et_3N (58 μmol, 8 μL). The compound was purified by column chromatography on silica gel (7/3 PE/EtOAc). All of the physical and spectroscopic data were in complete agreement with the reported ones.[22]

*4,9-Dihydroxy-1-methyl-1H-phenalene-2-carbaldehyde (**3i**).* According to the described general procedure, 586 mg (46%) of **3i** (red solid) was obtained from 2,7-dihydroxy-1-naphthtaldehyde (5.32 mmol, 1 g), catalyst (1.06 mmol, 345 mg), (*E*)-but-2-enal (10.62 mmol, 0.91 mL), and Et_3N (0.27 mmol, 37 μL). The compound was purified by column chromatography on silica gel (6/4 PE/EtOAc). All of the physical and spectroscopic data were in complete agreement with the reported ones.[22]

*Synthesis of Dimethoxy Phenalene Derivatives (**4aa–ia**).* Under an argon atmosphere, the naphthol derivative (1 equiv) was dissolved in anhydrous DMF (0.6 mol L^{-1}). K_2CO_3 (2 equiv) and then MeI (2.2 equiv) were added. The reaction mixture was stirred at room temperature for 5 h and then diluted with Et_2O. This resulting mixture was filtered and washed with Et_2O. The filtrate was washed with brine, dried over anhydrous Na_2SO_4, and evaporated under reduced pressure. The crude compound was purified by column chromatography on silica gel to afford the corresponding product.

*4,9-Dimethoxy-1-phenyl-1H-phenalene-2-carbaldehyde (**4aa**).* According to the described general procedure, 1.86 g (91%) of **4aa** (orange solid) was obtained from 4,9-dihydroxy-1-phenyl-1*H*-phenalene-2-carbaldehyde (**3a**) (6.25 mmol, 1.5 g), K_2CO_3 (12.50 mmol, 1.73 g), and MeI (13.75 mmol, 0.86 mL). The compound was purified by column chromatography on silica gel (7/3 PE/EtOAc). All of the physical and spectroscopic data were in complete agreement with the reported ones.[22]

*4,9-Dimethoxy-1-(p-tolyl)-1H-phenalene-2-carbaldehyde (**4ba**).* According to the described general procedure, 269 mg (90%) of **4ba** (orange solid) was obtained from 4,9-dihydroxy-1-(*p*-tolyl)-1*H*-phenalene-2-carbaldehyde (**3b**) (0.87 mmol, 275 mg), K_2CO_3 (1.74 mmol, 240 mg), and MeI (1.91 mmol, 120 μL). The compound was purified by column chromatography on silica gel (7/3 PE/EtOAc). R_f = 0.34 (PE/EtOAc 7/3). Mp 283−285 °C. ^{1}H NMR (300 MHz, acetone-d_6) δ 2.16 (s, 3H), 3.82 (s, 3H), 4.09 (s, 3H), 5.60 (s, 1H), 6.91−6.88 (m, 2H), 7.08−7.04 (m, 2H), 7.22 (d, *J* = 8.9 Hz, 1H), 7.32 (d, *J* = 9.2 Hz, 1H), 7.76 (d, *J* = 8.9 Hz, 1H), 7.94 (d, *J* = 9.2 Hz, 1H), 7.98 (s, 1H), 9.60 (s, 1H). ^{13}C{^{1}H} NMR (75 MHz, acetone-d_6) δ 20.9, 39.0, 56.3, 56.8, 111.8, 112.8, 115.0, 121.8, 124.5, 128.9 (3C), 129.2 (2C), 130.9, 134.2, 136.1, 138.2, 139.9, 142.8, 156.8, 157.0, 192.1. IR (ATR, cm^{-1}) 2938, 2712, 1661, 1263, 1252, 1158, 1055. HRMS (ES+) *m*/*z*: [M + Na]$^+$ calcd for $C_{23}H_{20}NaO_3$ 367.1310; found 367.1310.

*4,9-Dimethoxy-1-(4-methoxyphenyl)-1H-phenalene-2-carbaldehyde (**4ca**).* According to the described general procedure, 241 mg (74%) of **4ca** (orange solid) was obtained from 4,9-dihydroxy-1-(4-methoxyphenyl)-1*H*-phenalene-2-carbaldehyde (**3c**) (0.90 mmol, 300 mg), K_2CO_3 (1.80 mmol, 249 mg), and MeI (1.98 mmol, 285 μL). The compound was purified by column chromatography on silica gel (9/1 PE/EtOAc). R_f = 0.26 (PE/EtOAc 9/1). Mp 183−185 °C. ^{1}H NMR (300 MHz, $CDCl_3$) δ 3.69 (s, 3H), 3.79 (s, 3H), 4.05 (s, 3H), 5.65 (s, 1H), 6.68−6.63 (m, 2H), 7.07 (d, *J* = 8.9 Hz, 1H), 7.11 (d, *J* = 9.1 Hz, 1H), 7.16−7.14 (m, 2H), 7.63 (d, *J* = 8.9 Hz, 1H), 7.80 (d, *J* = 9.1 Hz, 1H), 7.94 (s, 1H), 9.58 (s, 1H). ^{13}C{^{1}H} NMR (75 MHz, $CDCl_3$) δ 37.9, 55.1, 56.0, 56.3, 110.5, 112.1, 113.2 (2C), 114.5, 121.6, 123.5, 127.7, 129.2 (2C), 130.1, 133.1, 137.0, 138.1, 139.0, 155.6, 156.0, 157.8, 192.2. IR (ATR, cm^{-1}) 3006, 2934, 2743, 1718, 1505, 1244, 1165. HRMS (ASAP+) *m*/*z*: [M + H]$^+$ calcd for $C_{23}H_{21}O_4$ 361.1440; found 361.1429.

*4,9-Dimethoxy-1-(3-methoxyphenyl)-1H-phenalene-2-carbaldehyde (**4da**).* According to the described general procedure, 566 mg (70%) of **4da** (yellow solid) was obtained from 4,9-dihydroxy-1-(3-methoxyphenyl)-1*H*-phenalene-2-carbaldehyde (**3d**) (2.08 mmol, 750 mg), K_2CO_3 (4.16 mmol, 574 mg), and MeI (4.58 mmol, 260 μL). The compound was purified by column chromatography on silica gel (7/3 PE/EtOAc). R_f = 0.4 (PE/EtOAc 7/3). Mp 155−157 °C. ^{1}H NMR (300 MHz, $CDCl_3$) δ 3.70 (s, 3H), 3.79 (s, 3H), 4.04 (s, 3H), 5.70 (s, 1H), 6.61 (ddd, *J* = 8.2, 2.5, 1.1 Hz, 1H), 6.85−6.82 (m, 2H), 7.05−7.01 (m, 1H), 7.07 (d, *J* = 8.9 Hz, 1H), 7.11 (d, *J* = 9.1 Hz, 1H), 7.64 (d, *J* = 8.9 Hz, 1H), 7.80 (d, *J* = 9.1 Hz, 1H), 7.95 (s, 1H), 9.59 (s, 1H). ^{13}C{^{1}H} NMR (75 MHz, $CDCl_3$) δ 38.0, 55.2, 56.1, 56.4, 110.6, 112.2, 113.2 (2C), 114.6, 121.7, 123.6, 127.8, 129.3 (2C), 130.3, 133.3, 137.1, 138.2, 139.2, 155.7, 156.2, 157.9, 192.3. IR (ATR, cm^{-1}) 2949, 2834, 1667, 1584, 1279, 1256, 1160, 1040. HRMS (ES+) *m*/*z*: [M + Na]$^+$ calcd for $C_{23}H_{20}NaO_4$ 383.1259; found 383.1247.

*4,9-Dimethoxy-1-(2-methoxyphenyl)-1H-phenalene-2-carbaldehyde (**4ea**).* According to the described general procedure, 120 mg (90%) of **4ea** (yellow solid) was obtained from 4,9-dihydroxy-1-(2-methoxyphenyl)-1*H*-phenalene-2-carbaldehyde (**3e**) (0.37 mmol, 124 mg), K_2CO_3 (0.74 mmol, 102 mg), and MeI (0.81 mmol, 48 μL). The compound was purified by column chromatography on silica gel (6/4 PE/EtOAc). R_f = 0.33 (PE/EtOAc 6/4). Mp 191−193 °C. ^{1}H NMR (300 MHz, $CDCl_3$) δ 3.70 (s, 6H), 4.04 (s, 3H), 5.99 (s, 1H), 6.71 (td, *J* = 14.6, 8.5, 4.6 Hz, 1H), 6.79 (d, *J* = 8.4 Hz, 1H), 7.13−7.00 (m, 4H), 7.59 (d, *J* = 8.4 Hz, 1H), 7.77 (d, *J* = 9.1 Hz, 1H), 7.97 (s, 1H), 9.55 (s, 1H). ^{13}C{^{1}H} NMR (75 MHz, $CDCl_3$) δ 34.0, 56.1 (2C), 56.3, 110.5, 111.7, 112.3, 114.9, 120.4, 122.1, 123.5, 127.2, 127.4, 130.5, 130.9, 132.7, 133.3, 138.1, 138.7, 155.2, 156.0, 157.1, 192.3. IR (ATR, cm^{-1}) 3020, 2949, 1656, 1595, 1205, 1292, 1103, 1090. HRMS (ES+) *m*/*z*: [M + Na]$^+$ calcd for $C_{23}H_{20}NaO_4$ 383.1530; found 383.1515.

*1-(4-Fluorophenyl)-4,9-dimethoxy-1H-phenalene-2-carbaldehyde (**4fa**).* According to the described general procedure, 400 mg (95%) of **4fa** (yellow solid) was obtained from 4,9-dihydroxy-1-(4-fluorophenyl)-1*H*-phenalene-2-carbaldehyde (**3f**) (1.21 mmol, 389 mg), K_2CO_3 (2.42 mmol, 334 mg), and MeI (2.66 mmol, 170 μL). The compound was purified by column chromatography on silica gel (7/3 PE/EtOAc). R_f = 0.37 (PE/EtOAc 7/3). Mp 195−197 °C. ^{1}H NMR (300 MHz, acetone-d_6) δ 3.83 (s, 3H), 4.10 (s, 3H), 5.62 (s, 1H), 6.90−6.82 (m, 2H), 7.21−7.15 (m, 2H), 7.23 (d, *J* = 8.9 Hz, 1H), 7.33 (d, *J* = 9.2 Hz, 1H), 7.79 (d, *J* = 8.9 Hz, 1H), 7.96 (d, *J* = 9.2 Hz, 1H), 8.01 (s, 1H), 9.61 (s, 1H). ^{13}C{^{1}H} NMR (75 MHz, acetone-d_6) δ 38.7, 56.3, 56.8, 111.9, 112.8, 114.7, 114.9, 115.2, 121.3, 124.5, 129.2, 130.6, 130.7, 134.4, 138.5, 139.5, 141.9, 143.5, 157.0, 161.1, 164.5, 192.2. IR (ATR, cm^{-1}) 3011, 2940, 2841, 1657, 1631, 1505, 1264, 1157, 1046. HRMS (ES+) *m*/*z*: [M + H]$^+$ calcd for $C_{22}H_{18}FO_3$ 349.1240; found 349.1235.

*1-(4-Chlorophenyl)-4,9-dimethoxy-1H-phenalene-2-carbaldehyde (**4ga**).* According to the described general procedure, 302 mg (60%) of **4ga** (yellow solid) was obtained from 4,9-dihydroxy-1-(4-chlorophenyl)-1*H*-phenalene-2-carbaldehyde (**3g**) (1.38 mmol, 465 mg), K_2CO_3 (2.76 mmol, 381 mg), and MeI (3.04 mmol, 189 μL). The compound was purified by column chromatography on silica gel (7/3 PE/EtOAc). R_f = 0.34 (PE/EtOAc 7/3). Mp 201−203 °C. ^{1}H NMR (300 MHz, $CDCl_3$) δ 3.78 (s, 3H), 4.06 (s, 3H), 5.66 (s, 1H), 7.11−7.05 (m, 3H), 7.18−7.14 (m, 3H), 7.66 (d, *J* = 8.9 Hz, 1H), 7.82 (d, *J* = 9.1 Hz, 1H), 7.96 (s, 1H), 9.57 (s, 1H). ^{13}C{^{1}H} NMR (75 MHz, $CDCl_3$) δ 38.3, 55.9, 56.3, 110.5, 111.9, 114.2, 120.8, 123.5, 127.9 (2C), 128.1, 129.7 (2C), 130.1, 131.6, 133.4, 138.3, 138.5,

https://dx.doi.org/10.1021/acs.joc.0c01140
J. Org. Chem. 2020, 85, 10603−10616

143.1, 155.8, 156.0, 191.9. IR (ATR, cm^{-1}) 3008, 2934, 2744, 1662, 1632, 1260, 1163, 815. HRMS (ES+) m/z: $[M + Na]^+$ calcd for $C_{22}H_{17}ClNaO_3$ 387.0764; found 387.0760.

1-(4-Bromophenyl)-4,9-dimethoxy-1H-phenalene-2-carbaldehyde (4ha). According to the described general procedure, 234 mg (74%) of **4ha** (yellow solid) was obtained from 4,9-dihydroxy-1-(4-bromophenyl)-1*H*-phenalene-2-carbaldehyde (**3h**) (0.77 mmol, 294 mg), K_2CO_3 (1.54 mmol, 213 mg), and MeI (1.69 mmol, 105 μL). The compound was purified by column chromatography on silica gel (7/3 PE/EtOAc). R_f = 0.41 (PE/EtOAc 7/3). Mp 196−198 °C. ^{1}H NMR (300 MHz, $CDCl_3$) δ 3.83 (s, 3H), 4.10 (s, 3H), 5.69 (s, 1H), 7.11 (d, J = 8.9 Hz, 1H), 7.18−7.14 (m, 3H), 7.31−7.26 (m, 2H), 7.71 (d, J = 8.9 Hz, 1H), 7.87 (d, J = 9.2 Hz, 1H), 8.01 (s, 1H), 9.61 (s, 1H). $^{13}C\{^1H\}$ NMR (75 MHz, $CDCl_3$) δ 37.9, 55.5, 55.9, 110.1, 111.5, 113.8, 120.3, 123.0, 127.5 (2C), 127.7, 129.3 (2C), 129.7, 131.2, 133.0, 137.9, 138.1, 142.7, 155.4, 155.6, 191.5. IR (ATR, cm^{-1}) 2932, 2856, 1665, 1632, 1503, 1252, 1161, 579. HRMS (ES+) m/z: $[M + H]^+$ calcd for $C_{22}H_{18}BrO_3$ 409.0439; found 409.0421.

4,9-Dimethoxy-1-methyl-1H-phenalene-2-carbaldehyde (4ia). According to the described general procedure, 337 mg (86%) of **4ia** (yellow solid) was obtained from 4,9-dihydroxy-1-methyl-1*H*-phenalene-2-carbaldehyde (**3i**) (1.46 mmol, 350 mg), K_2CO_3 (2.92 mmol, 404 mg), and MeI (3.21 mmol, 200 μL). The compound was purified by column chromatography on silica gel (9/1 cyclohexane/EtOAc). R_f = 0.33 (cyclohexane/EtOAc 9/1). Mp 148−149 °C. ^{1}H NMR (300 MHz, $CDCl_3$) δ 1.25 (d, J = 6.7 Hz, 3H), 3.96 (s, 3H), 4.01 (s, 3H), 4.61 (q, J = 6.7 Hz, 1H), 7.06 (d, J = 9.1 Hz, 1H), 7.15 (d, J = 8.9 Hz, 1H), 7.63 (d, J = 8.9 Hz, 1H), 7.76 (d, J = 9.1 Hz, 1H), 7.85 (s, 1H), 9.65 (s, 1H). $^{13}C\{^1H\}$ NMR (75 MHz, $CDCl_3$) δ 22.5, 27.9, 55.9, 56.3, 110.5, 111.6, 114.8, 123.0, 123.7, 127.1, 130.2, 132.9, 138.9, 140.9, 155.1, 155.4, 192.7. IR (ATR, cm^{-1}) 2977, 2938, 2839, 1654, 1510, 1255, 1169, 1044. HRMS (ES+) m/z: $[M + H]^+$ calcd for $C_{17}H_{17}O_3$ 269.1178; found 269.1173.

Synthesis of 4,9-bis(Benzyloxy)-1-phenyl-1H-phenalene-2-carbaldehyde (4ab). Under an argon atmosphere, 4,9-dihydroxy-1-phenyl-1*H*-phenalene-2-carbaldehyde (**3a**) (0.99 mmol, 300 mg, 1 equiv) and 4 mL of anhydrous acetone were added into a flask. K_2CO_3 (2.5 mmol, 346 mg, 2.5 equiv) and benzyl bromide (2.5 mmol, 0.30 mL, 2.5 equiv) were then added. The reaction mixture was left to stir at reflux using a round-bottom flask heating block for 5 h at which point the mixture was cooled down to room temperature and 10 mL of dichloromethane was then added. The resulting mixture was then filtered through a pad of celite and washed with dichloromethane. The filtrate was evaporated under reduced pressure. The compound was purified by column chromatography on silica gel (8/2 PE/EtOAc) to afford the corresponding product **4ab** as a yellow solid (316 mg, 66%). R_f = 0.28 (PE/EtOAc 8/2). Mp 222−224 °C. ^{1}H NMR (300 MHz, $CDCl_3$) δ 5.00 (d, J = 12.0 Hz, 1H), 5.11 (d, J = 12.0 Hz, 1H), 5.30 (d, J = 11.9 Hz, 1H), 5.35 (d, J = 11.9 Hz, 1H), 5.74 (s, 1H), 7.14−7.05 (m, 6H), 7.21−7.16 (m, 3H), 7.32−7.27 (m, 3H), 7.52−7.39 (m, 5H), 7.59 (d, J = 9.0 Hz, 1H), 7.76 (d, J = 9.0 Hz, 1H), 7.97 (s, 1H), 9.55 (s, 1H). $^{13}C\{^1H\}$ NMR (75 MHz, $CDCl_3$) δ 39.1, 70.2, 71.3, 112.1, 112.8, 115.3, 121.6, 123.6, 126.0, 127.4 (2C), 127.5 (2C), 127.7, 127.8 (2C), 127.9, 128.3, 128.4 (2C), 128.7 (2C), 128.8 (2C), 130.5, 133.0, 136.5, 136.7, 138.2, 139.0, 144.3, 154.8, 154.9, 192.1. IR (ATR, cm^{-1}) 2848, 1633, 1472, 1442, 1046. HRMS (ES+) m/z: $[M + H]^+$ calcd for $C_{34}H_{27}O_3$ 483.1960; found 483.1964.

Synthesis of 4,9-bis(Allyloxy)-1-phenyl-1H-phenalene-2-carbaldehyde (4ac). Under an argon atmosphere, 4,9-dihydroxy-1-phenyl-1*H*-phenalene-2-carbaldehyde (**3a**) (0.99 mmol, 300 mg, 1 equiv) and 4 mL of anhydrous acetone were added into a flask. K_2CO_3 (2.50 mmol, 345 mg, 2.5 equiv) and allyl bromide (3.96 mmol, 0.37 mL, 4 equiv) were then added. The reaction mixture was left to stir at reflux using a round-bottom flask heating block for 5 h. The solvent was removed under reduced pressure. The crude compound was purified by chromatography on silica gel (6/4 PE/EtOAc) to afford the corresponding product **4ac** as a yellow solid (250 mg, 65%). R_f = 0.42 (PE/EtOAc 6/4). Mp 147−149 °C. ^{1}H NMR (300 MHz, $CDCl_3$) δ 4.58−4.41 (m, 2H), 4.80−4.78 (m, 2H), 5.19−5.17 (m, 1H), 5.25−5.20 (m, 1H), 5.40−5.36 (m, 1H), 5.54−5.48 (m, 1H), 5.74 (s, 1H), 5.87 (ddt, J = 17.3, 10.4, 5.2 Hz, 1H), 6.16 (ddt, J = 17.3, 10.4, 5.2 Hz, 1H), 7.14−7.01 (m, 6H), 7.27−7.24 (m, 1H), 7.60 (d, J = 8.9 Hz, 1H), 7.77 (d, J = 9.1 Hz, 1H), 7.98 (s, 1H), 9.59 (s, 1H). $^{13}C\{^1H\}$ NMR (75 MHz, $CDCl_3$) δ 39.0, 69.3, 69.9, 111.8, 113.0, 115.0, 117.5, 118.2, 121.8, 123.6, 126.1, 127.6, 127.7 (2C), 128.5 (2C), 130.4, 133.0 (2C), 133.1, 138.3, 139.0, 144.4, 154.7, 155.0, 192.1. IR (ATR, cm^{-1}) 3060, 2862, 1665, 1631, 1262, 910. HRMS (ES+) m/z: $[M + H]^+$ calcd for $C_{26}H_{23}O_3$ 383.1647; found 383.1648.

Synthesis of 2-Formyl-1-phenyl-1H-phenalene-4,9-Diyl Diacetate (4ad). Under an argon atmosphere, 4,9-dihydroxy-1-phenyl-1*H*-phenalene-2-carbaldehyde (**3a**) (0.99 mmol, 300 mg, 1 equiv) and 8 mL of anhydrous pyridine were added into a flask. Acetic anhydride (3.96 mmol, 0.37 mL, 4 equiv) was then added. The reaction mixture was left to stir at room temperature for 5 h. The reaction mixture was poured into 100 mL of water and filtered. The solid was solubilized in 20 mL of ethyl acetate. The organic layer was then washed with 10 mL of 1 N HCl aq and 20 mL of saturated Na_2CO_3 aq and dried over anhydrous Na_2SO_4. The solvent was removed under reduced pressure to afford the product **4ad** as a yellow solid (192 mg, 50%). R_f = 0.42 (PE/EtOAc 7/3). Mp 175−177 °C. ^{1}H NMR (300 MHz, $CDCl_3$) δ 2.21 (s, 3H), 2.48 (s, 3H), 5.57 (s, 1H), 7.18−7.12 (m, 5H), 7.23 (d, J = 8.8 Hz, 1H), 7.30 (d, J = 9.0 Hz, 1H), 7.57 (s, 1H), 7.75 (d, J = 8.8 Hz, 1H), 7.89 (d, J = 9.0 Hz, 1H), 9.59 (s, 1H). $^{13}C\{^1H\}$ NMR (75 MHz, $CDCl_3$) δ 20.9, 21.1, 40.0, 120.2, 121.7, 123.2, 127.0, 127.2, 127.6, 128.3 (2C), 128.4 (2C), 129.1, 129.5, 132.1, 135.4, 140.9, 142.4, 146.9, 147.8, 168.5, 169.1, 191.5. IR (ATR, cm^{-1}) 3030, 2837, 1757, 1667, 1449, 1366, 1158, 1008. HRMS (ES+) m/z: $[M + H]^+$ calcd for $C_{24}H_{19}O_5$ 387.1232; found 387.1229.

Synthesis of 1-Phenyl-4,9-bis(prop-2-yn-1-yloxy)-1H-phenalene-2-carbaldehyde (4ae). Under an argon atmosphere, 4,9-dihydroxy-1-phenyl-1*H*-phenalene-2-carbaldehyde (**3a**) (4.3 mmol, 1.3 g, 1 equiv) and 19.5 mL of acetone were introduced into a flask. K_2CO_3 (8.6 mmol, 1.19 g, 2 equiv) and then propargyl bromide (22 mmol, 1.6 mL, 5 equiv) were added. The mixture was refluxed using a round-bottom flask heating block and stirred for 16 h. After the mixture was cooled to room temperature, 20 mL of dichloromethane was added. The organic layer was washed with NaOH 1 M aq and dried over anhydrous Na_2SO_4. The solvent was removed under reduced pressure to afford the product **4ae** as a yellow solid (1.17 g, 72%). R_f = 0.33 (PE/EtOAc 6/4). Mp 147−148 °C. ^{1}H NMR (400 MHz, acetone-d_6) δ 3.06 (t, J = 2.4 Hz, 1H), 3.20 (t, J = 2.4 Hz, 1H), 4.74 (dd, J = 15.8, 2.4 Hz, 1H), 4.83 (dd, J = 15.9, 2.4 Hz, 1H), 5.11 (d, J = 2.4 Hz, 2H), 5.67(s, 1H), 7.13−7.00 (m, 3H), 7.24−7.21 (m, 2H), 7.32 (d, J = 8.9 Hz, 1H), 7.42 (d, J = 9.2 Hz, 1H), 7.79 (d, J = 8.9 Hz, 1H), 7.96 (d, J = 9.2 Hz, 1H), 8.03 (s, 1H), 9.64 (s, 1H). $^{13}C\{^1H\}$ NMR (75 MHz, acetone-d_6) δ 39.6, 57.1, 57.8, 77.1, 77.9, 79.5, 79.6, 113.7, 114.3, 116.3, 122.9, 125.3, 126.9, 128.6 (2C), 128.8, 129.1 (2C), 130.8, 133.9, 138.0, 140.2, 145.2, 154.9, 155.2, 192.2. IR (ATR, cm^{-1}) 3262, 2124, 1660, 1634. HRMS (ASAP+) m/z: $[M + H]^+$ calcd for $C_{26}H_{19}O_3$ 379.1334; found 379.1336.

Synthesis of Phenalenone Derivatives 5−14. The protected compound **4** (1 equiv) and dichloromethane (0.02 mol L^{-1}) were introduced into a flask. MnO_2 (20 equiv) was then added. The reaction was left to stir at room temperature for 96 h. The reaction mixture was filtered through a pad of Celite and washed with dichloromethane, and the filtrate was then evaporated under reduced pressure. The crude compound was purified by column chromatography on silica gel (95/5 DCM/Et_2O) to afford the two isomers.

6-Methoxy-1-oxo-7-phenyl-1H-phenalene-8-carbaldehyde 5 and 6-Methoxy-1-oxo-9-phenyl-1H-phenalene-8-carbaldehyde 5′. According to the described general procedure, 707 mg (50%) of **5** (yellow solid) and 283 mg (20%) of **5′** (orange solid) were obtained from 4,9-dimethoxy-1-phenyl-1*H*-phenalene-2-carbaldehyde (**4aa**) (4.5 mmol, 1.5 g) and MnO_2 (90 mmol, 7.8 g). For **5**, R_f = 0.38 (DCM/Et_2O 95/5). Mp 232−234 °C. ^{1}H NMR (300 MHz, $CDCl_3$) δ 3.52 (s, 3H), 6.66 (d, J = 9.7 Hz, 1H), 6.85 (d, J = 8.1 Hz, 1H), 7.30−7.27 (m, 2H), 7.46−7.43 (m, 3H), 7.72 (d, J = 9.7 Hz, 1H), 7.78 (d, J = 8.1 Hz, 1H), 9.20 (s, 1H), 9.78 (s, 1H). $^{13}C\{^1H\}$ NMR (75 MHz, $CDCl_3$) δ 55.7, 107.0, 121.1, 123.4, 126.3, 127.5 (3C), 128.5, 128.6 (2C), 129.5, 131.5, 133.2, 135.6, 138.4, 142.5, 149.8, 162.2, 185.0, 191.5. IR (ATR, cm^{-1}) 3049, 2864, 1679, 1638, 1572, 1449, 1391, 1263, 1221, 1052, 1007. HRMS (ES+) *m/z*: $[M + H]^+$ calcd for $C_{21}H_{15}O_3$ 315.1021; found 315.1025. For **5′**, R_f = 0.58 (DCM/Et_2O 95/5). Mp decomposition. ^1H NMR (300 MHz, $CDCl_3$) δ 4.15 (s, 3H). 6.45 (d, J = 9.7 Hz, 1H), 6.96 (d, J = 8.0 Hz, 1H), 7.31−7.28 (m, 2H), 7.53−7.46 (m, 3H), 7.61 (d, J = 9.7 Hz, 1H), 7.81 (d, J = 8.0 Hz, 1H), 9.30 (s, 1H), 9.80 (s, 1H). $^{13}C\{^1H\}$ NMR (75 MHz, $CDCl_3$) δ 56.3, 105.1, 121.5, 124.5, 126.9, 127.5, 128.2 (3C), 128.5 (2C), 128.6, 131.5, 133.3, 135.6, 137.7, 140.2, 148.2, 160.7, 185.5, 191.7. IR (ATR, cm^{-1}) 3020, 2949, 2861, 1725, 1629, 1560, 1490, 1463, 1378, 1225, 1152. HRMS (ES+) *m/z*: $[M + H]^+$ calcd for $C_{21}H_{15}O_3$ 315.1021; found 315.1027.

6-(Benzyloxy)-1-oxo-7-phenyl-1H-phenalene-8-carbaldehyde ***6*** *and 6-(Benzyloxy)-1-oxo-9-phenyl-1H-phenalene-8-carbaldehyde* ***6′***. According to the described general procedure, 71 mg (55%) of **6** (yellow solid) and 12.9 mg (10%) of **6′** (yellow solid) were obtained from 4,9-bis(benzyloxy)-1-phenyl-1*H*-phenalene-2-carbaldehyde (**4ab**) (0.33 mmol, 134 mg) and MnO_2 (6.6 mmol, 574 mg). For **6**, R_f = 0.39 (DCM/Et_2O 95/5). Mp decomposition. ^1H NMR (300 MHz, $CDCl_3$) δ 4.85 (s, 2H), 6.67 (d, J = 9.7 Hz, 1H), 6.94 (d, J = 8.2 Hz, 1H), 6.99−6.96 (m, 2H), 7.13−7.08 (m, 1H), 7.25−7.17 (m, 5H), 7.29−7.28 (m, 2H), 7.72 (d, J = 9.7 Hz, 1H), 7.75 (d, J = 8.2 Hz, 1H), 9.20 (s, 1H), 9.67 (s, 1H). $^{13}C\{^1H\}$ NMR (75 MHz, $CDCl_3$) δ 71.2, 108.0, 121.1, 123.3, 126.3, 127.4 (2C), 127.6, 128.1 (2C), 128.2, 128.5 (5C), 129.5, 131.6, 133.4, 134.5, 135.5, 138.0, 142.5, 149.8, 161.2, 185.0, 191.5. IR (ATR, cm^{-1}) 3038, 2870, 1675, 1633, 1568, 1513, 1338, 1220, 1139. HRMS (ES+) *m/z*: $[M + Na]^+$ calcd for $C_{27}H_{18}NaO_3$ 413.1154; found 413.1150. For **6′**, R_f = 0.63 (DCM/Et_2O 95/5). ^1H NMR (300 MHz, $CDCl_3$) δ 5.41 (s, 2H), 6.45 (d, J = 9.7 Hz, 1H), 7.02 (d, J = 8.0 Hz, 1H), 7.31−7.28 (m, 2H), 7.47−7.40 (m, 5H), 7.55−7.48 (m, 3H), 7.60 (d, J = 9.7 Hz, 1H), 7.77 (d, J = 8.0 Hz, 1H), 9.35 (s, 1H), 9.80 (s, 1H).

6-(Allyloxy)-1-oxo-7-phenyl-1H-phenalene-8-carbaldehyde ***7*** *and 6-(Allyloxy)-1-oxo-9-phenyl-1H-phenalene-8-carbaldehyde* ***7′***. According to the described general procedure, 178 mg (50%) of **7** (yellow solid) and 29 mg (8%) of **7′** (yellow solid) were obtained from 4,9-bis(allyloxy)-1-phenyl-1*H*-phenalene-2-carbaldehyde (**4ac**) (0.83 mmol, 400 mg) and MnO_2 (16.6 mmol, 1.4 g). For **7**, R_f = 0.35 (DCM/Et_2O 95/5). Mp 167−169 °C. ^1H NMR (300 MHz, $CDCl_3$) δ 4.30 (d, J = 5.5 Hz, 2H), 5.11−5.04 (m, 2H), 5.31−5.18 (m, 1H), 6.64 (d, J = 9.7 Hz, 1H), 6.84 (d, J = 8.1 Hz, 1H), 7.29−7.27 (m, 2H), 7.44−7.41 (m, 3H), 7.70 (d, J = 9.7 Hz, 1H), 7.75 (d, J = 8.1 Hz, 1H), 9.18 (s, 1H), 9.73 (s, 1H). $^{13}C\{^1H\}$ NMR (75 MHz, $CDCl_3$) δ 53.4, 69.7, 107.8, 118.4, 121.1, 123.4, 126.2, 127.5, 127.7 (2C), 128.4, 128.7 (2C), 129.5, 131.6, 133.2, 135.6, 138.5, 142.5, 149.8, 161.1, 184.9, 191.5. IR (ATR, cm^{-1}) 3057, 2876, 2780, 1675, 1631, 1567, 1629, 1228, 1056, 1025. HRMS (ASAP+) *m/z*: $[M + H]^+$ calcd for $C_{23}H_{17}O_3$ 341.1178; found 341.1178. For **7′**, R_f = 0.55 (DCM/Et_2O 95/5). ^1H NMR (300 MHz, $CDCl_3$) δ 4.87−4.85 (m, 2H), 5.43 (dd, J = 10.5, 1.2 Hz, 1H), 5.56 (dd, J = 10.5, 1.2 Hz, 1H), 6.20 (ddt, J = 17.2, 10.5, 5.3 Hz, 1H), 6.45 (d, J = 9.6 Hz, 1H), 6.94 (d, J = 8.1 Hz, 1H), 7.29 (dd, J = 7.1, 1.6 Hz, 2H), 7.54−7.46 (m, 3H), 7.60 (d, J = 9.6 Hz, 1H), 7.78 (d, J = 8.1 Hz, 1H), 9.32 (s, 1H), 9.80 (s, 1H).

1-Oxo-7-phenyl-6-(prop-2-yn-1-yloxy)-1H-phenalene-8-carbaldehyde ***8*** *and 1-Oxo-9-phenyl-6-(prop-2-yn-1-yloxy)-1H-phenalene-8-carbaldehyde* ***8′***. According to the described general procedure, 206.6 mg (50%) of **8** (yellow solid) and 18.6 mg (5%) of **8′** (orange solid) were obtained from 1-phenyl-4,9-dipropynyl-1*H*-phanelene-2-carbaldehyde (**4ae**) (2.65 mmol, 1 g) and MnO_2 (53 mmol, 4.6 g). For **8**, R_f = 0.32 (DCM/Et_2O 95/5). Mp 188−191 °C. ^1H NMR (400 MHz, $CDCl_3$) δ 2.41 (t, J = 2.4 Hz, 1H), 4.37 (d, J = 2.4 Hz, 2H), 6.65 (d, J = 9.7 Hz, 1H), 7.00 (d, J = 8.1 Hz, 1H), 7.31−7.28 (m, 2H), 7.46−7.43 (m, 3H), 7.71 (d, J = 9.7 Hz, 1H), 7.78 (d, J = 8.1 Hz, 1H), 9.16 (s, 1H), 9.76 (s, 1H). $^{13}C\{^1H\}$ NMR (100 MHz, $CDCl_3$) δ 56.2, 76.4, 77.0, 108.9, 122.0, 123.8, 126.8, 127.8 (3C), 128.6, 128.9 (2C), 129.6, 131.7, 133.6, 135.1, 138.3, 142.4, 149.8, 159.8, 185.0, 191.5. IR (ATR, cm^{-1}) 3304, 2133, 1675, 1630, 1566, 1268. HRMS (ES+) *m/z*: $[M + H]^+$ calcd for $C_{23}H_{15}O_3$ 339.1021; found 339.1021. For **8′**, R_f = 0.47 (DCM/Et_2O 95/5). ^1H NMR (300 MHz, $CDCl_3$) δ 2.63 (t, J = 2.4 Hz, 1H), 5.04 (d, J = 2.4 Hz, 2H), 6.46 (d, J = 9.6 Hz, 1H), 7.10 (d, J = 8.1 Hz, 1H), 7.30−7.27 (m, 2H), 7.52−7.47 (m, 3H), 7.62 (d, J = 9.6 Hz, 1H), 7.81 (d, J = 8.1 Hz, 1H), 9.28 (s, 1H), 9.80 (s, 1H).

6-Methoxy-1-oxo-7-(p-tolyl)-1H-phenalene-8-carbaldehyde ***9*** *and 6-Methoxy-1-oxo-9-(p-tolyl)-1H-phenalene-8-carbaldehyde* ***9′***. According to the described general procedure, 135 mg (58%) of **9** (orange solid) and 33 mg (14%) of **9′** (orange solid) were obtained from 4,9-dimethoxy-1-(*p*-tolyl)-1*H*-phenalene-2-carbaldehyde (**4ba**) (0.71 mmol, 244 mg) and MnO_2 (14.2 mmol, 1.23 g). For **9**, R_f = 0.35 (DCM/Et_2O 95/5). Mp 256−258 °C. ^1H NMR (300 MHz, $CDCl_3$) δ 2.47 (s, 3H), 3.54 (s, 3H), 6.66 (d, J = 9.7 Hz, 1H), 6.85 (d, J = 8.1 Hz, 1H), 7.17−7.15 (m, 2H), 7.27−7.26 (m, 2H), 7.72 (d, J = 9.7 Hz, 1H), 7.77 (d, J = 8.1 Hz, 1H), 9.19 (s, 1H), 9.78 (s, 1H). $^{13}C\{^1H\}$ NMR (75 MHz, $CDCl_3$) δ 21.3, 55.7, 107.0, 121.1, 123.6, 126.3, 128.1 (2C), 128.5, 128.6 (2C), 129.4, 131.5, 133.5, 135.3, 135.5, 137.1, 142.4, 150.1, 162.3, 185.0, 191.7. IR (ATR, cm^{-1}) 3042, 2960, 2936, 1681, 1639, 1569, 1546, 1453, 1392. HRMS (ASAP+) *m/z*: $[M + H]^+$ calcd for $C_{22}H_{17}O_3$ 329.1178; found 329.1176. For **9′**, R_f = 0.52 (DCM/Et_2O 95/5). ^1H NMR (300 MHz, $CDCl_3$) δ 2.46 (s, 3H), 4.14 (s, 3H), 6.44 (d, J = 9.7 Hz, 1H), 6.95 (d, J = 8.1 Hz, 1H), 7.20−7.16 (m, 2H), 7.34−7.30 (m, 2H), 7.60 (d, J = 9.7 Hz, 1H), 7.79 (d, J = 8.1 Hz, 1H), 9.27 (s, 1H), 9.83 (s, 1H).

6-Methoxy-7-(4-methoxyphenyl)-1-oxo-1H-phenalene-8-carbaldehyde ***10*** *and 6-Methoxy-9-(4-methoxyphenyl)-1-oxo-1H-phenalene-8-carbaldehyde* ***10′***. According to the described general procedure, 53 mg (53%) of **10** (yellow solid) and 22 mg (22%) of **10′** (orange solid) were obtained from 4,9-dimethoxy-1-(4-methoxyphenyl)-1*H*-phenalene-2-carbaldehyde (**4ca**) (0.29 mmol, 104 mg) and MnO_2 (5.8 mmol, 504 mg). For **10**, R_f = 0.32 (DCM/Et_2O 95/5). Mp 228−230 °C. ^1H NMR (300 MHz, $CDCl_3$) δ 3.57 (s, 3H), 3.91 (s, 3H), 6.62 (d, J = 9.7 Hz, 1H), 6.85 (d, J = 8.1 Hz, 1H), 7.01−6.96 (m, 2H), 7.21−7.16 (m, 2H), 7.69 (d, J = 9.7 Hz, 1H), 7.76 (d, J = 8.1 Hz, 1H), 9.15 (s, 1H), 9.79 (s, 1H). $^{13}C\{^1H\}$ NMR (75 MHz, $CDCl_3$) δ 55.4, 55.8, 107.0, 112.9 (2C), 121.0, 123.6, 126.1, 128.5, 129.3, 130.0 (2C), 130.4, 131.5, 133.7, 135.6, 142.5, 149.7, 159.1, 162.4, 185.0, 191.8. IR (ATR, cm^{-1}) 3031, 2954, 2873, 1726, 1676, 1568, 1512, 1448, 1390, 1229, 1174. HRMS (ES+) *m/z*: $[M + H]^+$ calcd for $C_{22}H_{17}O_4$ 345.1127; found 345.1149. For **10′**, R_f = 0.65 (DCM/Et_2O 95/5). ^1H NMR (300 MHz, $CDCl_3$) δ 3.90 (s, 3H), 4.13 (s, 3H), 6.45 (d, J = 9.6 Hz, 1H), 6.93 (d, J = 8.1 Hz, 1H), 7.07−7.02 (m, 2H), 7.24− 7.19 (m, 2H), 7.59 (d, J = 9.6 Hz, 1H), 7.79 (d, J = 8.1 Hz, 1H), 9.25 (s, 1H), 9.85 (s, 1H).

6-Methoxy-7-(3-methoxyphenyl)-1-oxo-1H-phenalene-8-carbaldehyde ***11*** *and 6-Methoxy-9-(3-methoxyphenyl)-1-oxo-1H-phenalene-8-carbaldehyde* ***11′***. According to the described general procedure, 397 mg (57%) of **11** (yellow solid) and 84 mg (12%) of **11′** (orange solid) were obtained from 4,9-dimethoxy-1-(3-methoxyphenyl)-1*H*-phenalene-2-carbaldehyde (**4da**) (1.03 mmol, 400 mg) and MnO_2 (20.6 mmol, 1.79 g). For **11**, R_f = 0.4 (95/5 DCM/Et_2O). Mp 170−172 °C. ^1H NMR (300 MHz, $CDCl_3$) δ 3.56 (s, 3H), 3.83 (s, 3H), 6.63 (d, J = 9.7 Hz, 1H), 6.88−6.81 (m, 3H), 6.98 (ddd, J = 8.3, 2.6, 0.8 Hz, 1H), 7.35 (t, J = 7.9 Hz, 1H), 7.70 (d, J = 9.7 Hz, 1H), 7.77 (d, J = 8.3 Hz, 1H), 9.16 (s, 1H), 9.78 (s, 1H). $^{13}C\{^1H\}$ NMR (75 MHz, $CDCl_3$) δ 55.4, 55.8, 107.0, 113.0, 114.5, 121.0, 121.4, 123.3, 126.2, 128.3, 128.6, 129.5, 131.4, 133.1, 135.6, 139.7, 142.5, 149.4, 159.0, 162.2, 184.9, 191.5. IR (ATR, cm^{-1}) 2947, 2843, 1683, 1635, 1570, 1221, 1169, 1096, 1041. HRMS (ES+) *m/z*: $[M + H]^+$ calcd for $C_{22}H_{17}O_4$ 345.1127; found 345.1118. For **11′**, R_f = 0.65 (95/5 DCM/Et_2O). ^1H NMR (300 MHz, $CDCl_3$) δ 3.83 (s, 3H), 4.14 (s, 3H), 6.45 (d, J = 9.6 Hz, 1H), 6.83−6.82 (m, 1H), 6.88 (dt, J = 7.4, 1.2 Hz, 1H), 6.95 (d, J = 8.0 Hz, 1H), 7.00 (ddd, J = 8.4, 2.6, 1.2 Hz, 1H), 7.44−7.40 (m, 1H), 7.61 (d, J = 9.6 Hz, 1H), 7.80 (d, J = 8.0 Hz, 1H), 9.28 (s, 1H), 9.81 (s, 1H).

7-(4-Fluorophenyl)-6-methoxy-1-oxo-1H-phenalene-8-carbaldehyde ***12*** *and 9-(4-Fluorophenyl)-6-methoxy-1-oxo-1H-phenalene-8-carbaldehyde* ***12′***. According to the described general procedure, 114 mg (60%) of **12** (yellow solid) and 21 mg (11%) of **12′** (orange solid) were obtained from 1-(4-fluorophenyl)-4,9-dimethoxy-1*H*-

phenalene-2-carbaldehyde (**4fa**) (0.57 mmol, 200 mg) and MnO_2 (11.4 mmol, 991 mg). For **12**, R_f = 0.35 (DCM/Et_2O 95/5). Mp 240−241 °C. ^1H NMR (300 MHz, $CDCl_3$) δ 3.56 (s, 3H), 6.66 (d, J = 9.7 Hz, 1H), 6.87 (d, J = 8.1 Hz, 1H), 7.21−7.13 (m, 2H), 7.29−7.24 (m, 2H), 7.71 (d, J = 9.7 Hz, 1H), 7.78 (d, J = 8.1 Hz, 1H), 9.18 (s, 1H), 9.80 (s, 1H). $^{13}C\{^1H\}$ NMR (75 MHz, $CDCl_3$) δ 55.8, 107.1, 114.5, 114.8, 121.2, 123.5, 126.3, 128.5, 129.7, 130.3, 130.4, 131.5, 133.4, 134.2, 134.3, 135.6, 142.4, 148.5, 162.0, 184.8, 191.1. IR (ATR, cm^{-1}) 3066, 1682, 1634, 1220, 1094. HRMS (ES+) m/z: $[M + H]^+$ calcd for $C_{21}H_{14}FO_3$ 333.0927; found 333.0929. For **12′**, R_f = 0.61 (DCM/Et_2O 95/5). ^1H NMR (300 MHz, $CDCl_3$) δ 4.12 (s, 3H), 6.42 (d, J = 9.6 Hz, 1H), 6.94 (d, J = 8.1 Hz, 1H), 7.16−7.12 (m, 2H), 7.63−7.58 (m, 3H), 7.80 (d, J = 8.1 Hz, 1H), 9.27 (s, 1H), 9.80 (s, 1H).

*7-(4-Chlorophenyl)-6-methoxy-1-oxo-1H-phenalene-8-carbaldehyde **13** and 9-(4-Chlorophenyl)-6-methoxy-1-oxo-1H-phenalene-8-carbaldehyde **13′**.* According to the described general procedure, 83 mg (35%) of **13** (yellow solid) and 47 mg (20%) of **13′** (orange solid) were obtained from 1-(4-chlorophenyl)-4,9-dimethoxy-1*H*-phenalene-2-carbaldehyde (**4ga**) (0.75 mmol, 250 mg) and MnO_2 (15 mmol, 1.3 g). For **13**, R_f = 0.38 (DCM/Et_2O 95/5). Mp decomposition. ^1H NMR (300 MHz, $CDCl_3$) δ 3.57 (s, 3H), 6.67 (d, J = 9.7 Hz, 1H), 6.87 (d, J = 8.1 Hz, 1H), 7.25−7.22 (m, 2H), 7.48−7.43 (m, 2H), 7.73 (d, J = 9.7 Hz, 1H), 7.79 (d, J = 8.1 Hz, 1H), 9.19 (s, 1H), 9.80 (s, 1H). $^{13}C\{^1H\}$ NMR (75 MHz, $CDCl_3$) δ 55.8, 107.1, 121.1, 123.3, 126.3, 127.8 (2C), 128.4, 129.7 (2C), 130.0, 131.4, 133.1, 133.6, 135.7, 136.9, 142.5, 148.1, 161.9, 184.8, 190.9. IR (ATR, cm^{-1}) 3042, 1681, 1639, 1223, 829. HRMS (ES+) m/z: $[M + H]^+$ calcd for $C_{21}H_{14}ClO_3$ 349.0631; found 349.0629. For **13′**, R_f = 0.55 (DCM/Et_2O 95/5). ^1H NMR (300 MHz, $CDCl_3$) δ 4.15 (s, 3H), 6.45 (d, J = 9.7 Hz, 1H), 6.97 (d, J = 8.0 Hz, 1H), 7.25−7.21 (m, 2H), 7.51−7.47 (m, 2H), 7.63 (d, J = 9.7 Hz, 1H), 7.82 (d, J = 8.0 Hz, 1H), 9.30 (s, 1H), 9.82 (s, 1H).

*7-(4-Bromophenyl)-6-methoxy-1-oxo-1H-phenalene-8-carbaldehyde **14** and 9-(4-Bromophenyl)-6-methoxy-1-oxo-1H-phenalene-8-carbaldehyde **14′**.* According to the described general procedure, 54 mg (42%) of **14** (yellow solid) and 19 mg (15%) of **14′** (orange solid) were obtained from 1-(4-bromophenyl)-4,9-dimethoxy-1*H*-phenalene-2-carbaldehyde (**4ha**) (0.33 mmol, 134 mg) and MnO_2 (6.6 mmol, 574 mg). For **14**, R_f = 0.32 (DCM/Et_2O 95/5). Mp decomposition. ^1H NMR (300 MHz, $CDCl_3$) δ 3.57 (s, 3H), 6.67 (d, J = 9.8 Hz, 1H), 6.87 (d, J = 8.1 Hz, 1H), 7.21−7.16 (m, 2H), 7.63−7.59 (m, 2H), 7.72 (d, J = 9.8 Hz, 1H), 7.79 (d, J = 8.1 Hz, 1H), 9.19 (s, 1H), 9.80 (s, 1H). $^{13}C\{^1H\}$ NMR (75 MHz, $CDCl_3$) δ 55.8, 107.1, 121.2, 121.6, 123.3, 126.4, 128.5, 129.7, 130.3 (2C), 130.7 (2C), 131.5, 133.1, 135.6, 137.4, 142.5, 148.1, 161.9, 184.8, 190.9. IR (ATR, cm^{-1}) 3054, 2948, 1731, 1681, 1569, 1486, 1223, 1174, 1096, 805. HRMS (ES+) m/z: $[M + H]^+$ calcd for $C_{21}H_{14}BrO_3$ 393.0126; found 393.0115. For **14′**, R_f = 0.64 (DCM/Et_2O 95/5). ^1H NMR (300 MHz, $CDCl_3$) δ 4.15 (s, 3H), 6.45 (d, J = 9.7 Hz, 1H), 6.97 (d, J = 8.1 Hz, 1H), 7.20−7.15 (m, 2H), 7.65−7.61 (m, 3H), 7.83 (d, J = 8.1 Hz, 1H), 9.30 (s, 1H), 9.82 (s, 1H).

Photooxygenation of Anthracene 15. To a Schlenk flask were added anthracene **15** (0.28 mmol, 50 mg, 1 equiv), 6-methoxy-1-oxo-7-phenyl-1*H*-phenalene-8-carbaldehyde **5** (5.6 μmol, 1.76 mg, 2 mol %), methyl phenyl sulfone as an internal standard (0.14 mmol, 21.9 mg, 0.5 equiv), and $CDCl_3$ (3.5 mL) to give a yellow solution. The reaction medium was bubbled for 5 min with dioxygen and was then left under atmospheric pressure of dioxygen throughout the reaction time. The homogenous solution was irradiated with one blue LED (1 W, 25 lm, 470 nm typical wavelength). The distance from light source irradiation to the Schlenk vessel was 3 cm without the use of any filters. The reaction mixture was left to stir at room temperature, and an aliquot (0.2 mL) was taken from the reaction mixture at different reaction times. The aliquot was diluted with $CDCl_3$ (0.2 mL) and nitrogen was bubbled through the solution to remove oxygen. The samples were analyzed by ^1H NMR to determine the yield and product formation.

Photooxidation of Citronellol 17. To a Schlenk flask were added citronellol **17** (0.52 mmol, 95 μL, 1 equiv), 6-methoxy-1-oxo-7-phenyl-1*H*-phenalene-8-carbaldehyde **5** (10.40 μmol, 3.27 mg, 2 mol %), and $CHCl_3$ (2 mL) to give a yellow solution. The reaction medium was gently bubbled with dioxygen throughout the reaction time, and the homogenous solution was irradiated with one blue LED (1 W, 25 lm, 470 nm typical wavelength). The distance from light source irradiation to the Schlenk vessel was 3 cm without the use of any filters. The reaction mixture was left to stir at room temperature for 3 h at which point a saturated solution of $Na_2S_2O_3$ aq was added. Then, the reaction medium was left to stir at room temperature for 2 h. The solvent was removed under reduced pressure. The crude compound was purified by chromatography on silica gel (98/2 DCM/MeOH) to afford a 1:1 mixture of products **18a** and **18b** as a colorless oil (63 mg, 70%). R_f = 0.4 (mixture **18a** + **18b**, DCM/MeOH 98/2). ^1H NMR (300 MHz, $CDCl_3$) δ 0.91−0.88 (m, 6H), 1.27−1.02 (m, 2H), 1.30 (s, 6H, **18a**), 1.48−1.33 (m, 4H), 1.66−1.49 (m, 6H), 1.69−1.68 (m, 1H, **18a**), 1.71 (s, 3H, **18b**), 1.92 (dd, J = 6.6, 5.5 Hz) and 1.89−1.85 (m) (1H, **18a**), 2.05 (t, J = 5.5 Hz) and 2.02−1.99 (m) (1H, **18a**), 3.73−3.60 (m, 4H), 4.05−4.00 (m, 1H, **18b**), 4.82−4.81 (m, 1H, **18b**), 4.93−4.92 (m, 1H, **18b**), 5.60−5.57 (m, 2H, **18a**). All of the physical and spectroscopic data were in complete agreement with the reported ones.[32]

Photooxidation of Cyclohexa-1,3-diene 19. To a Schlenk flask were added cyclohexa-1,3-diene (**19**) (1 mmol, 80 mg, 1 equiv), 6-methoxy-1-oxo-7-phenyl-1*H*-phenalene-8-carbaldehyde (**5**) (20 μmol, 6.29 mg, 2 mol %), and $CHCl_3$ (4 mL) to give a yellow solution. The reaction medium was gently bubbled with dioxygen throughout the reaction time, and the homogenous solution was irradiated with one blue LED (1 W, 25 lm, 470 nm typical wavelength). The distance from light source irradiation to the Schlenk vessel was 3 cm without the use of any filters. The reaction mixture was left to stir at room temperature for 2 h at which point thiourea (1.26 mmol, 96 mg, 1 equiv) in 2 mL of MeOH was added. Then, the reaction mixture was vigorously left to stir at room temperature for 1 h. The reaction mixture was filtered through a pad of Celite and washed with MeOH. The solvent was removed under reduced pressure. The crude compound was purified by chromatography on silica gel (EtOAc) to afford the corresponding product **20** as a white solid (103 mg, 90%). R_f = 0.3 (EtOAc). ^1H NMR (300 MHz, $CDCl_3$) δ 1.85−1.75 (m, 4H), 4.15 (s, 2H), 5.86 (s, 2H). All of the physical and spectroscopic data were in complete agreement with the reported ones.[33]

Spectroscopic and Photophysical Measurements. UV−vis spectra were recorded on an Agilent 8453 Diode-Array spectrophotometer in the range of 250−700 nm. Emission spectra were recorded in an ISS PC1 spectrofluorometer at room temperature. Luminescence lifetime measurements were carried out using a PicoQuant FluoTime 200 fluorescence lifetime spectrometer with a multichannel scaler (PicoQuant's Timeharp 250) with the time-correlated single-photon counting (TCSPC) method. LEDs or lasers of adequate wavelength were employed as an excitation source. Fluorescence quantum yields were determined using eq 1 and 6-ethoxy-phenalenone in chloroform (Φ_F = 0.049) as a reference.[28]

$$\Phi_{F,sample} = \Phi_{F,reference}\frac{A_{reference}}{A_{sample}}\frac{I_{sample}}{I_{reference}}\left(\frac{\eta_{sample}}{\eta_{reference}}\right)^2 \quad (1)$$

Φ_F is the fluorescence quantum yields. A is the absorbance in the wavelength of excitation, I correspond to the area of the emission spectra, and η is the refractive index of the solvent.

Lifetime decays of singlet oxygen, $O_2(^1\Delta_g)$, were acquired with FluoTime 200 consisting of a multichannel scaler Nanoharp 200. Excitation at 355 nm was achieved with a laser FTSS355-Q3 (Crystal Laser, Berlin, Germany), working at 1 kHz repetition rate. For the detection at 1270 nm, an NIR PMT H10330A (Hamamatsu) was employed. The $O_2(^1\Delta_g)$ quantum yields (Φ_Δ) were determined by comparing the intensity at zero time of the 1270 nm signals to those of optically matched solutions of phenalenone as a reference, according to the following equation.[34]

$$\Phi_\Delta = \frac{I_\Delta(t=0)}{I'_\Delta(t=0)}\Phi'_\Delta$$

The transient difference absorption spectra and transient lifetimes were measured in an Edinburgh LP980 laser flash photolysis spectrometer. The excitation pump source was the Aurora II Integra 30 Nd:YAG/OPO system. The excitation wavelength was 355 nm (laser pulse ∼9 mJ, 8.2 ns) for all of the samples unless otherwise noted. A compact Peltier-cooled image-intensified charge coupled device (CCD) camera (ICCD Andor) was used to capture the whole spectrum in the presence and absence of the pump laser pulse. Each DOD spectrum was the average of 10 measurements. A Hamamatsu R928 side window photomultiplier was used for the kinetic measurements of DOD traces. For each measurement, optically diluted solutions were degassed by bubbling argon gas for about 20 min.

Computational Methods. All calculations reported here are based on density functional theory (DFT). Full gas-phase geometry optimizations of both phenalenone derivatives (namely **5** and **5′**) were performed using the hybrid B3LYP[35] exchange−correlation functional in conjunction with the split-valence double-ζ quality Def2SVP basis set for all atoms. Conformation analysis was also carried out in each derivative, identifying the most stables rotamers and the respective transition state connecting them. These stationary states were confirmed as local minima or first-order saddle points through a harmonic vibrational analysis in accord with the number of imaginary frequencies, zero or one, respectively. Using the rigid-rotor-harmonic-oscillator (RRHO) approximation at a given temperature, frequencies calculations also provide the thermal and entropic corrections for the free Gibbs energies ($G^{T}_{\mathrm{RRHO}}(B3LYP/Def2SVP)$). Additionally, more accurate electronic energies (E) for the rotameric changes were also computed at the same level of theory by single-point energy calculations combined with Def2TZVP. In those studies, solute−solvent interactions were described through the implicit SMD solvation model,[36] using methanol as a solvent. Therefore, the free Gibbs energy for each stationary state is given by

$$G = E + G^{\mathrm{T}}_{\mathrm{solv}} + G^{\mathrm{T}}_{\mathrm{RRHO}}$$

The excited features were investigated using the TD-DFT framework using the range-separated hybrid CAM-B3LYP[37] exchange−correlation functional combined with the split-valence triple-ζ quality Def2TZVP basis set at the gas-phase optimized geometries. All calculations were done employing the Gaussian09 suite of programs.[38] The CYLview program was used for molecular representations.[39]

■ ASSOCIATED CONTENT

Supporting Information

The Supporting Information is available free of charge at https://pubs.acs.org/doi/10.1021/acs.joc.0c01140.

Additional UV−vis and TRES spectra and fluorescence lifetimes of **5′** and computational details; copies of ^{1}H and ^{13}C spectra as well as full characterization (2D-NMR spectra) of **5** and **5′** (PDF)

■ AUTHOR INFORMATION

Corresponding Author

Vincent Coeffard − *CEISAM UMR CNRS 6230, Université de Nantes, F-44000 Nantes, France*; orcid.org/0000-0003-2982-7880; Email: vincent.coeffard@univ-nantes.fr

Authors

Paul De Bonfils − *CEISAM UMR CNRS 6230, Université de Nantes, F-44000 Nantes, France*

Elise Verron − *CEISAM UMR CNRS 6230, Université de Nantes, F-44000 Nantes, France*; orcid.org/0000-0003-4276-5127

Catalina Sandoval-Altamirano − *Facultad de Química y Biología, Universidad de Santiago de Chile, Santiago 518000, Chile*; orcid.org/0000-0002-8550-3218

Pablo Jaque − *Facultad de Ciencias Químicas y Farmacéuticas, Departamento de Química Orgánica y Fisicoquímica, Universidad de Chile, Santiago 8380492, Chile*; orcid.org/0000-0002-4055-3553

Xavier Moreau − *Institut Lavoisier de Versailles, Université Paris-Saclay, UVSQ, CNRS, 78035 Versailles, France*; orcid.org/0000-0002-6737-9671

German Gunther − *Facultad de Ciencias Químicas y Farmacéuticas, Departamento de Química Orgánica y Fisicoquímica, Universidad de Chile, Santiago 8380492, Chile*; orcid.org/0000-0002-4733-8426

Pierrick Nun − *CEISAM UMR CNRS 6230, Université de Nantes, F-44000 Nantes, France*; orcid.org/0000-0003-4501-0555

Complete contact information is available at: https://pubs.acs.org/10.1021/acs.joc.0c01140

Notes

The authors declare no competing financial interest.

■ ACKNOWLEDGMENTS

This work benefited from the support of the project CaROS ANR-18-CE07-0013-01 of the French National Research Agency (ANR). In particular, P.D.B. thanks ANR for a Ph.D. grant. We also thank Université de Nantes and CNRS for financial support. G.G. thanks FONDEQUIP EQM160099. Dr. Stéphane Diring is gratefully acknowledged for cyclic voltammetry.

■ REFERENCES

(1) (a) Yang, M.; Yang, T.; Mao, C. Enhancement of Photodynamic Cancer Therapy by Physical and Chemical Factors. *Angew. Chem., Int. Ed.* **2019**, *58*, 14066−14080. (b) Lan, M.; Zhao, S.; Liu, W.; Lee, C.-S.; Zhang, W.; Wang, P. Photosensitizers for Photodynamic Therapy. *Adv. Healthcare Mater.* **2019**, *8*, No. 1900132. (c) Li, X.; Kolemen, S.; Yoon, J.; Akkaya, E. U. Activatable Photosensitizers: Agents for Selective Photodynamic Therapy. *Adv. Funct. Mater.* **2017**, *27*, No. 1604053. (d) Fan, W.; Huang, P.; Chen, X. Overcoming the Achilles' heel of photodynamic therapy. *Chem. Soc. Rev.* **2016**, *45*, 6488−6519. (e) Kamkaew, A.; Lim, S. H.; Lee, H. B.; Kiew, L. V.; Chung, L. Y.; Burgess, K. BODIPY dyes in photodynamic therapy. *Chem. Soc. Rev.* **2013**, *42*, 77−88. (f) Dolmans, D. E. J. G. J.; Fukumura, D.; Jain, R. K. Photodynamic therapy for cancer. *Nat. Rev. Cancer* **2003**, *3*, 380−387.

(2) (a) Winckler, K. D. Special section: Focus on anti-microbial photodynamic therapy (PDT). *J. Photochem. Photobiol., B* **2007**, *86*, 43−44. (b) Hamblin, M. R.; Hasan, T. Photodynamic therapy: a new antimicrobial approach to infectious disease? *Photochem. Photobiol. Sci.* **2004**, *3*, 436−450. (c) Jori, G.; Brown, S. B. Photosensitized inactivation of microorganisms. *Photochem. Photobiol. Sci.* **2004**, *3*, 403−405.

(3) (a) Calzavara-Pinton, P.; Rossi, M. T.; Sala, R.; Venturini, M. Photodynamic Antifungal Chemotherapy. *Photochem. Photobiol.* **2012**, *88*, 512−522. (b) Donnelly, R. F.; McCarron, P. A.; Tunney, M. M. Antifungal photodynamic therapy. *Microbiol. Res.* **2008**, *163*, 1−12.

(4) Wiehe, A.; O'Brien, J. M.; Senge, M. O. Trends and targets in antiviral phototherapy. *Photochem. Photobiol. Sci.* **2019**, *18*, 2565−2612.

(5) (a) Ogilby, P. R. Singlet oxygen: there is indeed something new under the sun. *Chem. Soc. Rev.* **2010**, *39*, 3181−3209. (b) Zamadar, M.; Greer, A. In Singlet Oxygen as a Reagent in Organic Synthesis. *Handbook of Synthetic Photochemistry*; Albini, A.; Fagnoni, M., Eds.;

Wiley-VCH Verlag GmbH & Co. KGaA: Weinheim, Germany, 2009; pp 353−386.

(6) (a) Baptista, M. S.; Cadet, J.; Di Mascio, P.; Ghogare, A. A.; Greer, A.; Hamblin, M. R.; Lorente, C.; Nunez, S. C.; Ribeiro, M. S.; Thomas, A. H.; Vignoni, M.; Yoshimura, T. M. Type I and Type II Photosensitized Oxidation Reactions: Guidelines and Mechanistic Pathways. *Photochem. Photobiol.* **2017**, *93*, 912−919. (b) . *Singlet Oxygen: Applications in Biosciences and Nanosciences*; Nonell, S.; Flors, C., Eds.; Comprehensive Series in Photochemical & Photobiological Sciences; Royal Society of Chemistry: Cambridge, 2016.

(7) Turro, N. J.; Ramamurthy, V.; Scaiano, J. C. *Principles of Molecular Photochemistry: an Introduction*; University Science Books: Sausalito, CA, 2009.

(8) Zhao, J.; Chen, K.; Hou, Y.; Che, Y.; Liu, L.; Jia, D. Recent progress in heavy atom-free organic compounds showing unexpected intersystem crossing (ISC) ability. *Org. Biomol. Chem.* **2018**, *16*, 3692−3701.

(9) (a) Oliveros, E.; Bossmann, S. H.; Nonell, S.; Martí, C.; Heit, G.; Tröscher, G.; Neuner, A.; Martínez, C.; Braun, A. M. Photochemistry of the singlet oxygen $[O_2(^1\Delta_g)]$ sensitizer perinaphthenone (phenalenone) in *N,N′*-dimethylacetamide and 1,4-dioxane. *New J. Chem.* **1999**, *23*, 85−93. (b) Martí, C.; Jürgens, O.; Cuenca, O.; Casals, M.; Nonell, S. Aromatic ketones as standards for singlet molecular oxygen $O_2(^1\Delta_g)$ photosensitization. Time-resolved photoacoustic and near-IR emission studies. *J. Photochem. Photobiol., A* **1996**, *97*, 11−18.

(10) Flors, C.; Nonell, S. Light and Singlet Oxygen in Plant Defense Against Pathogens: Phototoxic Phenalenone Phytoalexins. *Acc. Chem. Res.* **2006**, *39*, 293−300.

(11) For selected examples, see: (a) Jing, Y.; Xu, Q.; Chen, M.; Shao, X. Pyridone-containing phenalenone-based photosensitizer working both under light and in the dark for photodynamic therapy. *Bioorg. Med. Chem.* **2019**, *27*, 2201−2208. (b) Salmerón, M. L.; Quintana-Aguiar, J.; De La Rosa, J. V.; López-Blanco, F.; Castrillo, A.; Gallardo, G.; Tabraue, C. Phenalenone-photodynamic therapy induces apoptosis on human tumor cells mediated by caspase-8 and p38-MAPK activation. *Mol. Carcinog.* **2018**, *57*, 1525−1539. (c) Cieplik, F.; Wimmer, F.; Muehler, D.; Thurnheer, T.; Belibasakis, G. N.; Hiller, K.-A.; Maisch, T.; Buchalla, W. Phenalen-1-One-Mediated Antimicrobial Photodynamic Therapy and Chlorhexidine Applied to a Novel Caries Biofilm Model. *Caries Res.* **2018**, *52*, 447−453. (d) Muehler, D.; Sommer, K.; Wennige, S.; Hiller, K.-A.; Cieplik, F.; Maisch, T.; Späth, A. Light-activated phenalen-1-one bactericides: efficacy, toxicity and mechanism compared with benzalkonium chloride. *Future Microbiol.* **2017**, *12*, 1297−1310. (e) Tabenski, I.; Cieplik, F.; Tabenski, L.; Regensburger, J.; Hiller, K.-A.; Buchalla, W.; Maisch, T.; Späth, A. The impact of cationic substituents in phenalen-1-one photosensitizers on antimicrobial photodynamic efficacy. *Photochem. Photobiol. Sci.* **2016**, *15*, 57−68. (f) Späth, A.; Leibl, C.; Cieplik, F.; Lehner, K.; Regensburger, J.; Hiller, K.-A.; Bäumler, W.; Schmalz, G.; Maisch, T. Improving Photodynamic Inactivation of Bacteria in Dentistry: Highly Effective and Fast Killing of Oral Key Pathogens with Novel Tooth-Colored Type-II Photosensitizers. *J. Med. Chem.* **2014**, *57*, 5157−5168.

(12) Freijo, M. B.; López-Arencibia, A.; Piñero, J. E.; McNaughton-Smith, G.; Abad-Grillo, T. Design, synthesis and evaluation of amino-substituted 1H-phenalen-1-ones as anti-leishmanial agents. *Eur. J. Med. Chem.* **2018**, *143*, 1312−1324.

(13) Lazzaro, A.; Corominas, M.; Martí, C.; Flors, C.; Izquierdo, L. R.; Grillo, T. A.; Luis, J. G.; Nonell, S. Light- and singlet oxygen-mediated antifungal activity of phenylphenalenone phytoalexins. *Photochem. Photobiol. Sci.* **2004**, *3*, 706−710.

(14) Gutiérrez, D.; Flores, N.; Abad-Grillo, T.; McNaughton-Smith, G. Evaluation of Substituted Phenalenone Analogues as Antiplasmodial Agents. *Exp. Parasitol.* **2013**, *135*, 456−458.

(15) Phatangare, K. R.; Lanke, S. K.; Sekar, N. Phenalenone Fluorophores-Synthesis, Photophysical Properties and DFT Study. *J. Fluoresc.* **2014**, *24*, 1827−1840.

(16) For selected examples, see: (a) Ospina, F.; Ramirez, A.; Cano, M.; Hidalgo, W.; Schneider, B.; Otálvaro, F. Synthesis of Positional Isomeric Phenylphenalenones. *J. Org. Chem.* **2017**, *82*, 3873−3879. (b) Ospina, F.; Hidalgo, W.; Cano, M.; Schneider, B.; Otálvaro, F. Synthesis of 8-Phenylphenalenones: 2-Hydroxy-8-(4-hydroxyphenyl)-1*H*-phenalen-1-one from *Eichhornia crassipes*. *J. Org. Chem.* **2016**, *81*, 1256−1262. (c) Duque, L.; Zapata, C.; Rojano, B.; Schneider, B.; Otálvaro, F. Radical Scavenging Capacity of 2,4-Dihydroxy-9-phenyl-1*H*-phenalen-1-one: A Functional Group Exclusion Approach. *Org. Lett.* **2013**, *15*, 3542−3545. (d) Cano, M.; Rojas, C.; Hidalgo, W.; Sáez, J.; Gil, J.; Schneider, B.; Otálvaro, F. Improved synthesis of 4-phenylphenalenones: the case of isoanigorufone and structural analogs. *Tetrahedron Lett.* **2013**, *54*, 351−354. (e) Nanclares, J.; Gil, J.; Rojano, B.; Saez, J.; Schneider, B.; Otálvaro, F. Synthesis of 4-methoxy-1H-phenalen-1-one: a subunit related to natural phenalenone-type compounds. *Tetrahedron Lett.* **2008**, *49*, 3844−3847.

(17) (a) Tom, C. T. M. B.; Crellin, J. E.; Motiwala, H. F.; Stone, M. B.; Davda, D.; Walker, W.; Kuo, Y.-H.; Hernandez, J. L.; Labby, K. J.; Gomez-Rodriguez, L.; Jenkins, P. M.; Veatch, S. L.; Martin, B. R. Chemoselective ratiometric imaging of protein S-sulfenylation. *Chem. Commun.* **2017**, *53*, 7385−7388. (b) Buffet, N.; Grelet, E.; Bock, H. Soluble and Columnar Liquid Crystalline Peropyrenequinones by Coupling of Phenalenones in Caesium Hydroxide. *Chem. - Eur. J.* **2010**, *16*, 5549−5553. (c) Butera, J.; Bagli, J.; Doubleday, W.; Humber, L.; Treasurywala, A.; Loughney, D.; Sestanj, K.; Millen, J.; Sredy, J. Computer assisted design and synthesis of novel aldose reductase inhibitors. *J. Med. Chem.* **1989**, *32*, 757−765.

(18) Fukuyama, T.; Sugimori, T.; Maetani, S.; Ryu, I. Synthesis of perinaphthenones through rhodium-catalyzed dehydrative annulation of 1-naphthoic acids with alkynes. *Org. Biomol. Chem.* **2018**, *16*, 7583−7587.

(19) Lenk, R.; Tessier, A.; Lefranc, P.; Silvestre, V.; Planchat, A.; Blot, V.; Dubreuil, D.; Lebreton, J. 1-Oxo-1*H*-phenalene-2,3-dicarbonitrile Heteroaromatic Scaffold: Revised Structure and Mechanistic Studies. *J. Org. Chem.* **2014**, *79*, 9754−9761.

(20) For other synthetic strategies towards phenalenones, see: (a) Wang, M.-Z.; Ku, C.-F.; Si, T.-X.; Tsang, S.-W.; Lv, X.-M.; Li, X.-W.; Li, Z.-M.; Zhang, H.-J.; Chan, A. S. C. Concise Synthesis of Natural Phenylphenalenone Phytoalexins and a Regioisomer. *J. Nat. Prod.* **2018**, *81*, 98−105. (b) Yavari, I.; Khajeh-Khezri, A.; Halvagar, M. R. A Synthesis of Novel Perinaphthenones from Acetylenic Esters and Acenaphthoquinone−Malononitrile Adduct in the Presence of Triphenylphosphine. *Synlett* **2018**, *29*, 2011−2014. (c) Smith, A. B.; Kim, W.-S. Diversity-oriented synthesis leads to an effective class of bifunctional linchpins uniting anion relay chemistry (ARC) with benzyne reactivity. *Proc. Natl. Acad. Sci. U.S.A.* **2011**, *108*, 6787−6792.

(21) Briere, J.-F.; Lebeuf, R.; Levacher, V.; Hardouin, C.; Lecouve, J.-P. Novel method for the synthesis of 7-methoxy-naphthalene-1-carbaldehyde and use thereof in the synthesis of agomelatine. U.S. Patent WO2015082848A2, 2015.

(22) The best results were obtained by performing the aminocatalyzed reaction in the presence of diphenylprolinol silyl ether catalyst. See: Giardinetti, M.; Marrot, J.; Greck, C.; Moreau, X.; Coeffard, V. Aminocatalyzed Synthesis of Enantioenriched Phenalene Skeletons through a Friedel−Crafts/Cyclization Strategy. *J. Org. Chem.* **2018**, *83*, 1019−1025.

(23) For previous works dealing with oxidative dealkylation of polyenol ethers, see: (a) Zhao, G.; Xu, G.; Qian, C.; Tang, W. Efficient Enantioselective Syntheses of (+)-Dalesconol A and B. *J. Am. Chem. Soc.* **2017**, *139*, 3360−3363. (b) Hu, P.; Lee, S.; Park, K. H.; Das, S.; Herng, T. S.; Gonçalves, T. P.; Huang, K.-W.; Ding, J.; Kim, D.; Wu, J. Octazethrene and Its Isomer with Different Diradical Characters and Chemical Reactivity: The Role of the Bridge Structure. *J. Org. Chem.* **2016**, *81*, 2911−2919.

(24) Casellas, J.; Reguero, M. Photosensitization Versus Photocyclization: Competitive Reactions of Phenylphenalenone in Its Role as Phytoanticipins in Plant Defense Strategies. *J. Phys. Chem. A* **2018**, *122*, 811−821.

(25) Alberti, A.; Astolfi, P.; Carloni, P.; Greci, L.; Rizzolie, C.; Stipa, P. The reactivity of manganese dioxide towards different substrates in organic solvents. *New J. Chem.* **2015**, *39*, 8964−8970.
(26) Reid, D. Stable π-electron Systems and New Aromatic Structures. *Tetrahedron* **1958**, *3*, 339−352.
(27) Goto, K.; Kubo, T.; Yamamoto, K.; Nakasuji, K.; Sato, K.; Shiomi, D.; Takui, T.; Kubota, M.; Kobayashi, T.; Yakusi, K.; Ouyang, J. A Stable Neutral Hydrocarbon Radical: Synthesis, Crystal Structure, and Physical Properties of 2,5,8-Tri-*tert*-butyl-phenalenyl. *J. Am. Chem. Soc.* **1999**, *121*, 1619−1620.
(28) Sandoval-Altamirano, C.; De la Fuente, J. R.; Berrios, E.; Sanchez, S. A.; Pizarro, N.; Morales, J.; Gunther, G. Photophysical characterization of hydroxy and ethoxy phenalenone derivatives. *J. Photochem. Photobiol., A* **2018**, *353*, 349−357.
(29) Kuimova, M. K. Mapping viscosity in cells using molecular rotors. *Phys. Chem. Chem. Phys.* **2012**, *14*, 12671−12686.
(30) (a) Martínez, C. G.; Neumer, A.; Marti, C.; Nonell, S.; Braun, A. M.; Oliveros, E. Effect of the Media on the Quantum Yield of Singlet Oxygen ($O_2(^1\Delta_g)$) Production by 9*H*-Fluoren-9-one: Solvents and Solvent Mixtures. *Helv. Chim. Acta* **2003**, *86*, 384−397. For another example of solvent effect on singlet oxygen quantum yield, see: (b) Takizawa, S.; Breitenbach, T.; Westberg, M.; Holmegaard, L.; Gollmer, A.; Jensen, R. L.; Murata, S.; Ogilby, P. R. Solvent Dependent Photosensitized Singlet Oxygen Production from an Ir(iii) Complex: Pointing to Problems in Studies of Singlet-Oxygen-Mediated Cell Death. *Photochem. Photobiol. Sci.* **2015**, *14*, 1831−1843.
(31) (a) Fischer, J.; Serier-Brault, H.; Nun, P.; Coeffard, V. Substrate-Selectivity in Catalytic Photooxygenation Processes Using a Quinine-BODIPY System. *Synlett* **2020**, *31*, 463−468. (b) Fischer, J.; Mele, L.; Serier-Brault, H.; Nun, P.; Coeffard, V. Controlling Photooxygenation with a Bifunctional Quinine-BODIPY Catalyst: towards Asymmetric Hydroxylation of β-Dicarbonyl Compounds. *Eur. J. Org. Chem.* **2019**, *2019*, 6352−6358. (c) Mauger, A.; Farjon, J.; Nun, P.; Coeffard, V. One-Pot Synthesis of Functionalized Fused Furans via a BODIPY-Catalyzed Domino Photooxygenation. *Chem. - Eur. J.* **2018**, *24*, 4790−4793. (d) Wilkinson, F.; Helman, W. P.; Ross, A. B. Rate Constants for the Decay and Reactions of the Lowest Electronically Excited Singlet State of Molecular Oxygen in Solution. An Expanded and Revised Compilation. *J. Phys. Chem. Ref. Data* **1995**, *24*, 663−1021.
(32) Lévesque, F.; Seeberger, P. H. Highly Efficient Continuous Flow Reactions Using Singlet Oxygen as a "Green" Reagent. *Org. Lett.* **2011**, *13*, 5008−5011.
(33) Feng, K.; Wu, L.-Z.; Zhang, L.-P.; Tung, C.-H. IRA200 resin-supported platinum(II) complex for photooxidation of olefins. *Tetrahedron* **2007**, *63*, 4907−4911.
(34) Schmidt, R.; Tanielian, C.; Dunsbach, R.; Wolff, C. Phenalenone, a universal reference compound for the determination of quantum yields of singlet oxygen $O_2(^1\Delta_g)$ sensitization. *J. Photochem. Photobiol., A* **1994**, *79*, 11−17.
(35) (a) Becke, D. A. Density-functional thermochemistry. III. The role of exact exchange. *J. Chem. Phys.* **1993**, *98*, 5648−5652. (b) Lee, C.; Yang, W.; Parr, R. G. Development of the Colle-Salvetti correlation-energy formula into a functional of the electron density. *Phys. Rev. B* **1988**, *37*, 785−789.
(36) Marenich, A. V.; Cramer, C. J.; Truhlar, D. G. Universal Solvation Model Based on Solute Electron Density and on a Continuum Model of the Solvent Defined by the Bulk Dielectric Constant and Atomic Surface Tensions. *J. Phys. Chem. B* **2009**, *113*, 6378−6396.
(37) Yanai, T.; Tew, D.; Handy, N. A new hybrid exchange-correlation functional using the Coulomb-attenuating method (CAM-B3LYP). *Chem. Phys. Lett.* **2004**, *393*, 51−57.
(38) See Supporting Information for full reference.
(39) Legault, C. Y. CYLview, 1.0b. 2009, http://www.cylview.org.

https://dx.doi.org/10.1021/acs.joc.0c01140
J. Org. Chem. 2020, 85, 10603−10616